Developmental Biology **232,** 127–148 (2001)
doi:10.1006/dbio.2001.0155, available online at http://www.idealibrary.com on IDEAL®

metadata, citation and similar papers at core.ac.uk
brought to you by CORE
provided by Elsevier - Publisher Connector

Sperm Factor Initiates Capacitance and Conductance Changes in Mouse Eggs That Are More Similar to Fertilization Than IP_3- or Ca^{2+}-induced Changes

Sherwin C. Lee,* Rafael A. Fissore,† and Richard Nuccitelli*,[1]

**Section of Molecular and Cellular Biology, University of California, Davis, California 95616; and †Department of Veterinary and Animal Sciences, University of Massachusetts, Amherst, Massachusetts 01003*

We used patch clamp electrophysiology and concurrent imaging with the Ca^{2+}-sensitive dye, fura-2, to study the temporal relationship between membrane capacitance and conductance and intracellular free Ca^{2+} concentration ($[Ca^{2+}]_i$) during mouse egg fertilization. We found an ~2 pF step increase in egg membrane capacitance and a minor increase in conductance with no change in $[Ca^{2+}]_i$ at sperm fusion. This was followed ~1 min later by a rise in $[Ca^{2+}]_i$ that led to larger changes in capacitance and conductance. The most common pattern for these later capacitance changes was an initial capacitance decrease, followed by a larger increase and eventual return to the approximate starting value. There was some variation in this pattern, and sub-μM peak $[Ca^{2+}]_i$ favored capacitance decrease, while higher $[Ca^{2+}]_i$ favored capacitance increase. The magnitude of accompanying conductance increases was variable and did not correlate well with peak $[Ca^{2+}]_i$. The intracellular introduction of porcine sperm factor reproduced the postfusion capacitance and conductance changes with a similar $[Ca^{2+}]_i$ dependence. Raising $[Ca^{2+}]_i$ by the intracellular introduction of IP_3 initiated fertilization-like capacitance changes, but the conductance changes were slower to activate. Capacitance decrease could be induced when $[Ca^{2+}]_i$ was increased modestly by activation of an endogenous Ca^{2+} current, with little effect on resting conductance. These results suggest that net turnover of the mouse egg surface membrane is sensitive to $[Ca^{2+}]_i$ and that sperm and the active component of sperm factor may be doing more than initiating the IP_3-mediated release of intracellular Ca^{2+}. © 2001 Academic Press

Key Words: **patch clamp; exocytosis; endocytosis; fura-2; calcium imaging; calcium channel; ionomycin.**

INTRODUCTION

In all plant and animal eggs that have been studied, fertilization is accompanied by a rise in intracellular free Ca^{2+} concentration ($[Ca^{2+}]_i$) that usually spreads across the egg in a wave-like manner. There are currently three popular hypotheses to explain how the sperm produces this increase in the much larger egg cell: (1) The "calcium bomb" hypothesis proposes that upon fertilization Ca^{2+} enters the egg either from stores in the sperm itself or through channels in the sperm's plasma membrane and triggers calcium-induced calcium release from the ER in the egg (Jaffe, 1983). (2) The second hypothesis stipulates activation of a receptor on the egg surface as a result of specific sperm–egg binding (Evans and Kopf, 1998). (3) The third requires sperm–egg fusion to deliver a catalytic activity or sperm factor carried by the sperm (Swann, 1990). The latter two of these then lead to the production of IP_3, which is essential for the fertilization-induced release of Ca^{2+} from intracellular stores in mammalian eggs (Miyazaki *et al.*, 1993). In mammalian eggs, the most compelling evidence supports the sperm factor hypothesis, but contributions from other activation mechanisms are still possible.

One of the problems in dissecting out contributing elements is the difficulty of determining the exact moment of sperm–egg fusion and its temporal relation with the $[Ca^{2+}]_i$ increase and other events of egg activation. In hamster eggs, the fertilization-induced $[Ca^{2+}]_i$ increase appears to happen very quickly after sperm fusion. In contrast, mouse eggs appear to have a delay of ~1–5 min between sperm fusion and the initiation of a $[Ca^{2+}]_i$ increase. The best evidence for

[1] To whom correspondence should be addressed at Section of Molecular and Cellular Biology, One Shields Avenue, University of California, Davis, CA 95616-8535. Fax: 530-752-7522. E-mail: rlnuccitelli@ucdavis.edu.

0012-1606/01 $35.00
Copyright © 2001 by Academic Press
All rights of reproduction in any form reserved.

this comes from dye-transfer studies that showed cytoplasmic continuity between egg and sperm before the $[Ca^{2+}]_i$ rise (Lawrence *et al.*, 1997; Jones *et al.*, 1998). This delay has made it difficult to correlate sperm–egg fusion precisely with the other steps in mouse egg activation, but it also provides an opportunity to delineate the timing of various activation events if the instant of sperm fusion can be known.

Electrophysiological methods should be able to provide a good assay for sperm–egg interactions. In mammals, changes in membrane potential and some of the underlying conductances have been described for mouse (Igusa *et al.*, 1983; Jaffe *et al.*, 1983), hamster (Miyazaki and Igusa, 1981; 1982; Igusa *et al.*, 1983), rabbit (McCulloh *et al.*, 1983), and human (Gianaroli *et al.*, 1994) fertilization. Most of these are older studies that followed membrane potential with conventional microelectrode technology. Some more recent work has employed patch clamp methods to voltage clamp eggs and measure conductance changes directly (Gianaroli *et al.*, 1994; Dale *et al.*, 1996). None of these studies has noted any changes specific to the moment of sperm fusion. This suggests that any membrane potential or conductance changes are too small to be noticeable in this way or are quickly swamped by Ca^{2+}-dependent conductances attendant to the $[Ca^{2+}]_i$ increase.

Capacitance is a measure of membrane surface area and can be sensitively assayed under favorable conditions. Inasmuch as fertilization involves the fusion of sperm and egg membranes, sufficiently sensitive capacitance measurements could directly and rapidly assay this event. The capacitance of a patch of membrane on the surface of a sea urchin egg was monitored during fusion of a sperm with that patch, allowing the authors to mark the exact instant of sperm–egg fusion (McCulloh and Chambers, 1992). These unique data enabled them to conclude that a considerable early conductance increase coincident with fertilization is contributed by the sperm and that sperm–egg electrical continuity is a necessary prerequisite for sea urchin egg activation. However, technical difficulties with this preparation precluded the authors from following subsequent behavior of the patch for very long, and other work suggests that the details of mammalian sperm–egg interaction might be different. For example, sperm fusion in sea urchin is sensitive to egg membrane potential (Jaffe, 1976), but this appears not to be the case for mammals (Jaffe *et al.*, 1983; McCulloh *et al.*, 1983). In hamster, whole egg capacitance was monitored during fertilization and showed a very nice correlation between the activation of Ca^{2+}-dependent K^+ current and the increase of membrane surface area due to Ca^{2+}-dependent exocytosis of cortical granules (Kline and Stewart-Savage, 1994). However, these authors did not note the actual moment of fusion, probably because the very large surface area of the hamster egg and the early postfusion activation of K^+ current made it too difficult to see this very small change in capacitance.

Our initial goal in this work was to duplicate and expand upon the work of McCulloh and Chambers (1992) using eggs of the frog *Xenopus laevis*. Although it was possible to make cell-attached patch membrane recordings on these cells (with difficulty; see also Kline, 1986), it proved impossible to fertilize from within the patch pipet. Hoping to utilize another well-studied system where sperm are more efficient than *Xenopus*, we tried the same experiment with eggs of the fish medaka (*Oryzias latipes*); however, we were unable to obtain high-resistance patch electrode seals on this membrane.

Mouse eggs are a more favorable preparation for looking at sperm–egg fusion. Although the prospects for obtaining fertilization from within the patch pipet are daunting because of the large size and poor fusion efficiency of mouse sperm, the relatively smaller size of the mouse egg made it practical to do the study while monitoring the electrical properties of the entire egg surface. Even though the diameter of mouse eggs is only a little less than hamster, early estimates indicated that their surface area was only approximately one-third that of hamster (Georgiou *et al.*, 1984), probably because of many fewer microvilli. Moreover, the delay in the $[Ca^{2+}]_i$ increase and generally modest conductance changes at fertilization in mouse suggested that we might be able to see capacitance and conductance changes cleanly.

We report here that sperm fusion in mouse is indicated by an ~2 pF step increase in egg membrane capacitance and a minor increase in conductance. This is followed by a rise in $[Ca^{2+}]_i$ that initiates further, larger changes in capacitance and conductance. The most common postfusion capacitance changes are an initial capacitance decrease, followed by a larger increase and eventual return to the approximate starting value. There is some variation in this pattern depending on size of the $[Ca^{2+}]_i$ increase: a peak $[Ca^{2+}]_i$ increase that is sub-μM favors a capacitance decrease, while higher $[Ca^{2+}]_i$ favors capacitance increase. The magnitude of the accompanying conductance increase is variable, but the conductance change always appears as an increase of inward current from a holding potential of −40 mV. The postfusion changes in capacitance and conductance could be reproduced with a similar $[Ca^{2+}]_i$ dependence by intracellular introduction of porcine sperm factor or by exposure to calcium ionophore. However, a rise in $[Ca^{2+}]_i$ may not be the only factor in the postfusion membrane changes. Raising $[Ca^{2+}]_i$ by the intracellular introduction of IP_3 initiated the same capacitance changes as fertilization, but the conductance changes were somewhat different. Similarly, a capacitance decrease could also be produced when $[Ca^{2+}]_i$ was increased modestly by activation of an endogenous voltage-dependent Ca^{2+} current, with little effect on resting conductance. These results highlight the sensitivity to $[Ca^{2+}]_i$ of the mouse egg surface membrane and further suggest that sperm and the active component of sperm factor do more than initiate the IP_3-mediated release of intracellular Ca^{2+}.

Copyright © 2001 by Academic Press. All rights of reproduction in any form reserved.

METHODS

Gamete Preparation

All gametes were obtained from ICR mice in collaboration with the Myles/Primakoff Laboratory at this institution. The isolation, selection, and preparation of zona pellucida-free eggs and of capacitated/acrosome-reacted sperm was performed by standard methods as described previously (Faure *et al.*, 1999). Briefly, superovulation was induced in ICR mice (Harlan Sprague-Dawley, Indianapolis, IN) by a 5- to 10-IU injection of pregnant mare's serum gonadotropin followed 48 h later by a 5- to 10-IU injection of human chorionic gonadotropin (both from Sigma Chemical). Animals were sacrificed 12–14 h after the second injection, and cumulus masses containing eggs were isolated into warmed culture media (M199; GIBCO BRL, Rockville, MD) supplemented with 3.5 mM Na pyruvate, penicillin-streptomycin (GIBCO BRL), and 0.3% (w/v) bovine serum albumin (BSA; fraction V, cell culture tested; Sigma). Cumulus cells were removed by treatment for a few minutes with type I-S hyaluronidase (Sigma). *Zonae pellucidae* were removed from selected metaphase II eggs with one polar body by brief treatment with chymotrypsin (Sigma) and passage through a narrow bore pipet. Zona-free eggs were washed and stored in 100-μl drops of supplemented M199 under light mineral oil at 37°C in a humidified incubator with 5% CO_2 and 95% air.

Sperm were collected from the cauda epididymis and vas deferens of ICR mice. Released sperm were held in 100-μl drops of supplemented M199 (but with 3.0% BSA) in the same 37°C incubator for 3 h to allow spontaneous capacitation and acrosome reaction. Stock concentration was 1–5 $\times$ 10^6 sperm/ml; concentration as used was ~20–100 $\times$ 10^3 sperm/ml.

Experimental Conditions

Experiments were done in a chamber fashioned by sealing a 25-mm circular coverslip over a circular hole in a 35-mm plastic culture dish with Hi-Temp-Vac lubricant (VWR Scientific, San Francisco, CA). A 500-μl bath solution was placed on the glass and covered with light mineral oil. This solution was either BSA-free M2 Ringer (also without antibiotics or Phenol Red; after Hogan *et al.*, 1986) or a pyruvate-supplemented simple saline containing (in mM) 140 NaCl, 5 KCl, 2 $CaCl_2$, 1 $MgCl_2$, 0.33 Na pyruvate, 5.5 glucose, 10 Mops, pH 7.4.

The chamber was placed into a drilled out aluminum block through which heated water flowed from a circulating water bath (Lauda). In all imaging experiments and most nonimaging experiments as well, the bottom of the chamber was in contact with a 40$\times$ Nikon Fluor oil immersion objective that was wrapped in copper tubing containing the same circulating heated water. The temperature in the bath just above the objective was 35–38°C measured with a YSI thermocouple thermometer (Yellow Springs, OH).

Electrophysiology

Standard whole-cell and perforated-patch methods were used. Pipets were pulled on a Sutter P-97 puller (Novato, CA) from standard wall 1.5-mm OD borosilicate glass without filament (WPI, Sarasota, FL) and fire-polished lightly. Average pipet resistance was 3.0 $\pm$ 0.5 MΩ (SD, n = 86, median 2.9). The most common pipet fill solution contained (in mM) 115 potassium aspartate, 35 KCl (or 25 KCl and 10 NaCl), 1 K_2EGTA, 10 Mops (or Hepes), pH 7.2 at 275–280 mOsm; this was usually supplemented with 1 $MgCl_2$ and 1 K_2ATP for whole-cell recording. Perforated-patch pipets were filled with the same solution supplemented with 200 μg/ml Pluronic F-127 and 250 μg/ml nystatin. The bath was grounded via a thin glass tube containing saline in 2% agar leading from the central drop in the chamber to a saline reservoir containing a Ag/AgCl pellet.

Eggs were transferred directly from culture media to the recording chamber without an intervening wash. With the fine bore pipets used to move mammalian eggs, very little medium is transferred with the cells, and the small amount of BSA brought into the recording chamber did not interfere with the formation of GΩ seals. Surprisingly, we had no additional difficulty forming seals after moving our patch pipets through the overlaying oil, as long as light positive pressure was maintained in passing through the air/oil and oil/saline interfaces. Seals were established with gentle suction and seemed to be aided by a negative potential on the pipet. Seals of ~1–10 GΩ were achieved in a few seconds to a few minutes. Perforated-patch recordings often started showing patch permeabilization before a high seal resistance was realized; but the resistance generally continued to improve, or the recording was stopped. Whole-cell configuration was achieved usually with a sharp jolt of suction to rupture the patch.

About two-thirds of the recordings were made with a GeneClamp 500 amplifier (Axon Instruments, Foster City, CA) in patch mode with a CV-5–1G (low gain) headstage. Although this amplifier is not specifically designed for whole-cell patch recording, it was sufficient for our particular application because the method for measurement of capacitance that we utilized precludes the use of the amplifier-based corrections (membrane capacity compensation, series resistance compensation, etc.) that the GeneClamp does not have. We only used hardware compensation for the capacitance of the pipet (~3 pF). About one-third of the recordings were done with a Dagan 3900A amplifier (Dagan Corp., Minneapolis, MN) with indistinguishable results.

Almost all experiments performed for this study involved extended monitoring of membrane capacitance and resistance. This was done using the Membrane Test facility in pClamp 7 (Axon Instruments), which both reports in real-time and can save for later analysis membrane capacitance, membrane resistance, access resistance, and holding current. We used the in-routine averaging (50 "edges") such that the effective sampling rate in most experiments was ~1 Hz. The data files produced were transferred to Microsoft Excel (Microsoft Corp., Redmond, WA) for analysis and then to Igor Pro (WaveMetrics, Lake Oswego, OR) for the generation of figures. As presented in this paper, conductance is the simple inverse of the membrane resistance reported by pClamp, and capacitance is the pClamp capacitance value corrected for the shortfall of the test voltage step caused by the access resistance. This correction was less than 5% except for instances of low membrane resistance (large conductance) and/or high access resistance (e.g., some perforated-patch experiments). For fertilization and other lengthy procedures, we only included cells that we had confidence in for tens of minutes. Generally, we terminated recording or rejected eggs that developed large "leak" currents or exhibited increasing or unstable access resistance. Egg activation by itself did not affect seal quality or the integrity of the recording.

Calcium Imaging

Estimates of intracellular free Ca^{2+} concentration ($[Ca^{2+}]_i$) were made using the Ca^{2+}-sensitive dye fura-2. In most experiments,

Copyright © 2001 by Academic Press. All rights of reproduction in any form reserved.

TABLE 1
Patch-Clamped Mouse Egg Initial Parameters

	Initial Capacitance (pF)[a]	Initial Conductance (nS)	Lowest Conductance (nS)	Lowest Holding Current (pA)
Whole Cell	175.7 ± 29.6 (102) (Median 178.2)	5.9 ± 2.8 (Median 5.2)	4.8 ± 2.4 (Median 4.1)	−48 ± 90 (92) (Median −19)
Perforated	173.2 ± 33.4 (27) (Median 175.7)	7.1 ± 2.5 (Median 6.6)	4.5 ± 1.7 (Median 4.4)	−7 ± 56 (27) (Median +7)
Total	175.2 ± 30.3 (129) (Median 177.3)	6.1 ± 2.8 (Median 5.6)	4.8 ± 2.3 (Median 4.2)	−39 ± 85 (119) (Median −15)

[a] Values are presented as mean ± SD (no. of observations). All analysis was done in Microsoft Excel.

cells were loaded with dye by incubation for 30–60 min with 10 μM fura-2/AM under culture conditions. Eggs to be imaged were then transferred to the above described experimental chamber for concurrent imaging and electrophysiology. In some imaging experiments, the eggs were not preloaded with dye, but 0.2–0.26 mM of the free-acid form of fura-2 was included in the whole-cell pipet fill solution. When fura-2 was introduced from the pipet, the intensity of the dye signal in the egg would increase for 30 min or more after patch rupture, but there was usually enough signal to proceed with the experiment after 5–10 min.

Imaging was done using the software program, Ratiotool (Inovision Corp., Raleigh, NC), running on a Sun SparcStation 2 (Sun Microsystems, Mountain View, CA). A filter wheel was used to alternate between excitation at 350 and 385 nm; emission was at 510 nm. Each 350 and 385 image was captured and stored for later analysis. Each image was made with a 0.25-s exposure, and image pairs were acquired every 10 s in most experiments. For cells loaded with the free-acid form of fura-2, $[Ca^{2+}]_i$ was calculated directly from the background-corrected ratio of the 350/385 intensities according to the formula (Grynkiewicz *et al.*, 1985):

$$[Ca^{2+}]_i(\text{nM}) = 225 \times (R - R_{\min})/(R_{\max} - R) \times (s_{f,2}/s_{b,2}) \qquad [1]$$

where 225 is the K_d, R is the ratio of fluorescence intensity due excitation at 350 nm over that at 385 nm, $R_{\min}$ is the ratio Ca^{2+}-free, $R_{\max}$ is the ratio with calcium saturated, and $s_{f,2}/s_{b,2}$ is the ratio of fluorescence intensities for the fully free and fully bound dye for 385 excitation. Calibration was done *in vitro* in microcuvettes (VitroCom, Mountain Lakes, NJ) using Ca^{2+}-buffered, 150 mM $[K^+]$ solutions containing 0.1 mM fura-2, as described previously (Lee and Pappone, 1999). There was little evidence for dye compartmentation in cells loaded directly with fura-2 via the pipet. Both the 350 and 385 fluorescent signals behaved as expected with $[Ca^{2+}]_i$ changes; and, when the fura-2-containing pipet was removed from the cell, the 350 and 385 signals decreased in parallel.

However, dye compartmentation appeared to be a significant problem for cells loaded via the acetoxymethylester form of fura-2. The 350 intensity in these cells was found to be almost completely insensitive to changes in $[Ca^{2+}]_i$ imposed by ionophore or any other treatment. We interpreted this as evidence that a significant fraction of the dye was in compartments not influenced by changes in cytoplasmic $[Ca^{2+}]$. Since most intracellular compartments are believed to contain high free $[Ca^{2+}]$ relative to the cytoplasm, and since fura-2 saturates at a few μM $[Ca^{2+}]$ (where the 350 signal is at its maximum and the 385 signal is very small), increases in the 350 signal due to increases in $[Ca^{2+}]_i$ were apparently overwhelmed by the large signal coming from compartmentalized dye. However, as the 385 signal still showed large, appropriate changes in intensity, it seemed reasonable to conclude that essentially all the 385 signal reflected cytoplasmic $[Ca^{2+}]$ changes. We therefore assumed that we could still estimate $[Ca^{2+}]_i$ under these conditions, employing fura-2 as if it were a single-wavelength intensity dye, according to the formula:

$$[Ca^{2+}]_i(\text{nM}) = 225 \times (F_{\max} - F)/(F - F_{\min}) \qquad [2]$$

where F is the experimental fluorescent intensity, and $F_{\max}$ and $F_{\min}$ are the intensities at very low and very high $[Ca^{2+}]$, respectively. $F_{\max}$ and $F_{\min}$ were derived from the same in vitro calibration used for the free acid form of fura-2 described above. We fit an unperturbed section of the 385 trace to adjust $F_{\max}$ and $F_{\min}$ for dye leakage. For periods of a few minutes, we generally used a linear fit; if we had a longer section to use, we used an exponential decay if this gave a better fit. And, we further assumed that the initial $[Ca^{2+}]_i$ in unperturbed cells was ~100 nM. Although many assumptions are made in this analysis, we found it yielded $[Ca^{2+}]_i$ values that were consistent with estimates based on ratioed fura-2 in eggs in which dye was introduced from the pipet, and the results were consistent across experiments.

Average fluorescence intensities from ~50% of the central area of imaged cells were determined in the image acquisition program. These results were then transferred to Microsoft Excel for the calculation of $[Ca^{2+}]_i$ and synchronization with the electrophysiology data.

Reagents

Boar sperm factor was prepared essentially as described previously (Wu *et al.*, 1997). Stock concentrations were 10 or 30 μg/μl. The potassium salt of fura-2 and Pluronic F-127 were obtained from Molecular Probes (Eugene, OR). Nystatin was obtained from Fluka (Ronkonkoma, NY). All other reagents were from Sigma Chemical (St. Louis, MO).

RESULTS

Properties of Unstimulated Mouse Eggs

We used the Membrane Test facility in the software package pClamp 7 (Axon Instruments) to continuously monitor the membrane properties of voltage-clamped

Copyright © 2001 by Academic Press. All rights of reproduction in any form reserved.

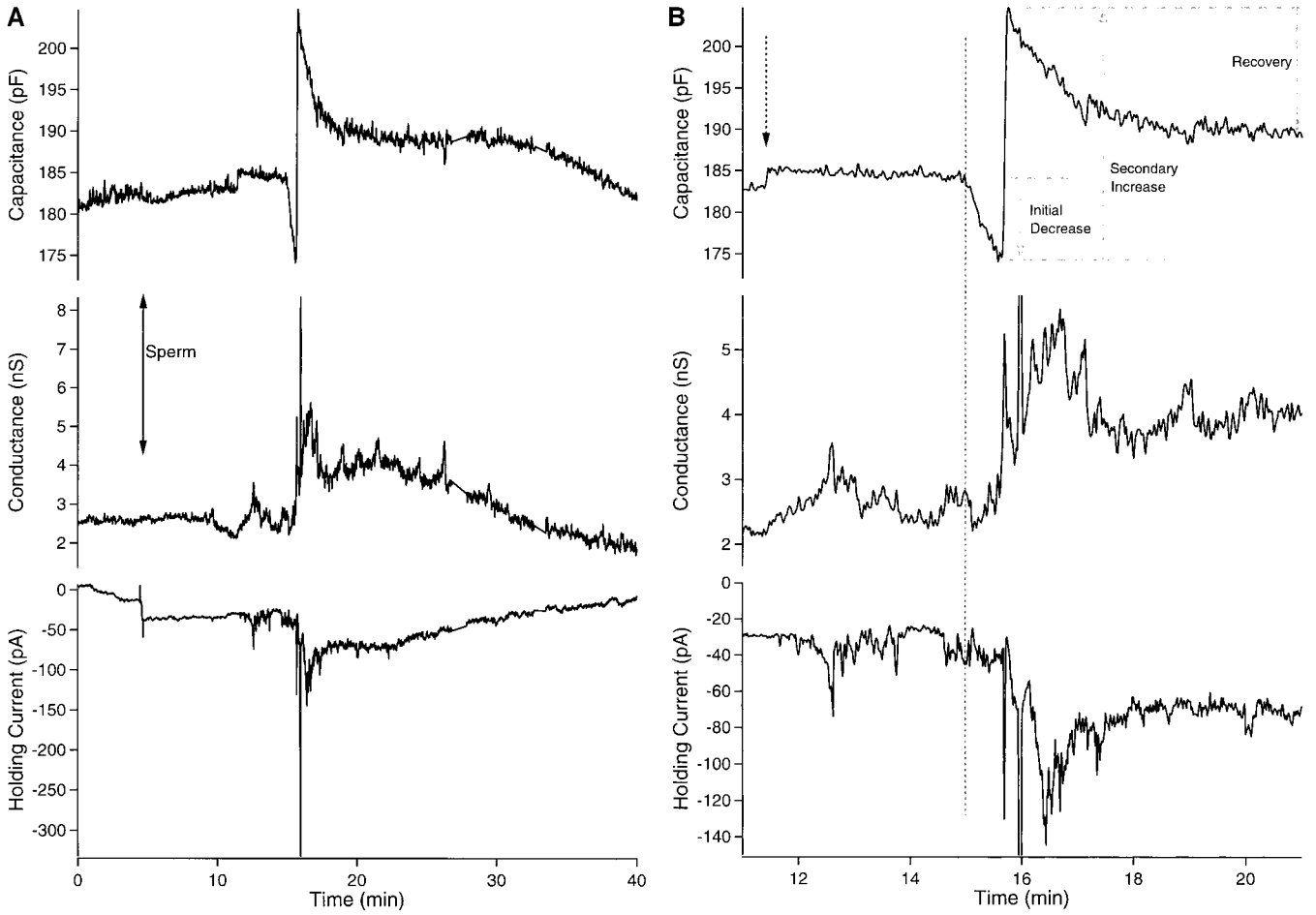

FIG. 1. Sperm-induced changes in membrane capacitance, conductance, and holding current. Zero time is from the point of patch rupture and entry into whole-cell patch configuration. Part A is the entire recording and part B is the specific period around fertilization. The double arrow line in A marks the addition of 10 μl of capacitated sperm suspension. In B, the dashed arrow marks the point of sperm fusion, and the dashed vertical line indicates the initiation of the fertilization-induced change in capacitance. The lighter dashed lines and arrows show how ΔC_m in Tables 2–5 was determined for Initial C_m decrease, Secondary C_m increase, and Recovery C_m. The bath solution was BSA-free M2 Ringer, and the pipet fill solution was our most-commonly used formulation (see Methods). Holding potential for this egg was −43 mV.

mouse eggs. The average initial capacitance was 175.2 ± 30.3 pF (SD, median 177.3 pF, n = 129; Table 1, range: 109 to 291 pF.) In whole-cell patch configuration, this value was determined usually within a few seconds of patch rupture. In perforated-patch configuration, the "start" point was 10–20 min after pipet contact and initiation of patch permeabilization. Both techniques gave equivalent results (Table 1). All capacitance values are corrected for access resistance as described in Methods.

The average initial membrane conductance was 6.1 ± 2.8 (SD) nS. The membrane conductance often decreased somewhat from this initial value; lowest membrane conductance measured in these cells was 4.8 ± 2.3 nS. This average input impedance of ~210 MΩ is somewhat higher than reported in earlier microelectrode studies of mouse eggs (Igusa *et al.*, 1983; Jaffe *et al.*, 1983). Again, there was no significant difference between whole-cell and perforated-patch configurations.

Almost all cells were voltage-clamped at or near −40 mV. This value was chosen because previous studies indicated this would be close to the actual membrane potential (Igusa *et al.*, 1983; Jaffe *et al.*, 1983; Peres, 1986). Although we did not make any systematic effort to verify this, our data gave generally low values for the holding current when eggs were clamped around −40 mV (Table 1), suggesting that this value is close to the resting level.

The intracellular Ca^{2+} concentration ($[Ca^{2+}]_i$) in unstimulated, whole-cell voltage-clamped mouse eggs as determined with the free acid form of fura-2 was 105 ± 37 nM (SD, n = 11, median was also 105). $[Ca^{2+}]_i$ in all unstimulated cells was very stable, but capacitance and conductance tended to change with time.

Copyright © 2001 by Academic Press. All rights of reproduction in any form reserved.

Capacitance showed a consistent pattern in patch-clamped eggs, especially in whole-cell configuration. The initial capacitance value would be stable for up to a few minutes and then begin a gradual decrease (see Figs. 2–5, but not Fig. 1). Often this would be a gradual change in slope, but sometimes there would be an inflection. This decrease could continue for tens of minutes before reaching a plateau and sometimes even reversing (see Figs. 4 and 5). Simple changes in the pipet fill solution (with or without ATP; 0, 1, or 10 mM EGTA; with or without 10 mM Na^+; all Cl^- in place of 115 mM aspartate$^-$) did not appear to affect this process. This pattern of capacitance change was also observed ~70% of the time in perforated-patch configuration. Very few eggs showed completely stable capacitance when monitored for more than a few minutes.

Similarly, the magnitude of the holding current was usually smallest at or near the beginning of the recording. After that, we generally observed some drift to larger negative (i.e., inward) currents. Small changes in holding current might not be reflected in an increase in conductance, and there was no consistent pattern to conductance changes in unstimulated cells. But all larger changes in conductance were strictly correlated with larger negative holding currents (Fig. 1).

Fertilization

Capacitance changes at fusion. Fertilization was attempted with 62 voltage-clamped mouse eggs. In 20 of these eggs, we observed characteristic changes in capacitance and conductance that we take to be indicative of successful fertilization. As shown in Figs. 1–3 and 5, fertilization is marked by a step increase in capacitance of ~2 pF a few minutes prior to a much larger capacitance oscillation (Table 2). We believe this step increase in capacitance represents the addition of sperm membrane to the egg plasma membrane at sperm fusion. The correlation between the 2-pF capacitance increase and egg activation is very strong. In no instance did we observe a 2-pF capacitance increase that was not followed by a larger capacitance oscillation. Visible sperm binding to the egg surface had no effect on egg capacitance or conductance. Four eggs showed two closely spaced capacitance steps preceding egg activation (e.g., Fig. 3), which we interpret as indicating that two sperm fused with these eggs. We did not observe any differences in these four cells compared to single-sperm fertilizations. Faure *et al.* (1999) observed a modest increase in the frequency of Ca^{2+} transients in polyspermic mouse eggs. Only one cell showed a large capacitance oscillation without a clear preceding fusion event (Fig. 4), and we observed no examples of fusion events occurring after activation.

Conductance changes at fusion. There is an increase in conductance associated with the 2-pF capacitance increase. This conductance change is generally more difficult to separate from the underlying signal noise and does not appear to come "on" as sharply as the capacitance change. In some instances, the conductance increase followed the capacitance increase (compare Figs. 3 and 5). On average, we estimate the conductance increase to be ~0.3 nS.

Fig. 1 is an example of the most common pattern of membrane changes that we observed during fertilization. Three minutes after the initial 2-pF step, there is a significant decrease in membrane capacitance followed by a larger, sharp increase and a slower return to the approximate starting value. This is accompanied by a conductance increase that initiates slightly behind the capacitance decrease and takes longer to recover. Changes in holding current mirror the conductance changes very closely.

$[Ca^{2+}]_i$ does not increase until 1–2 min after fusion. A sharp rise in $[Ca^{2+}]_i$ is the best studied and most commonly employed physiological marker for fertilization and egg activation. To assure ourselves that we were observing fertilization and to correlate the membrane changes we saw with changes in $[Ca^{2+}]_i$, we used concurrent Ca^{2+} imaging and electrophysiology. All the following experiments include an estimate of $[Ca^{2+}]_i$. There was no measurable change in $[Ca^{2+}]_i$ coincident with the presumptive sperm fusion event (Figs. 2-5). However, the earliest observable change following sperm fusion is a slow increase in $[Ca^{2+}]_i$ beginning ~1 min after the 2-pF capacitance increase. About 1–2 min after this, approximately coincident with a faster rise in $[Ca^{2+}]_i$, there are abrupt changes in capacitance and conductance that mark the onset of the membrane changes associated with egg activation (Figs. 2–5). The initiation of the capacitance change usually precedes the initiation of the conductance change by a few seconds. As our most consistent landmark, we used the time of the onset of this capacitance change as our reference time 0, as shown in Table 2. The average $[Ca^{2+}]_i$ at the start of the capacitance change is ~250 nM, and it is ~310 nM at the start of the conductance change.

Capacitance changes accompanying $[Ca^{2+}]_i$ increase. There are three different patterns of capacitance change observed during egg activation. These same patterns were observed in patch-clamped cells both with and without loading with fura-2. We are electing to present the data with concurrent Ca^{2+} imaging to highlight differences in $[Ca^{2+}]_i$ that may underlie differences in cell response. In the most prevalent capacitance pattern (Figs. 1 and 2), an initial capacitance decrease is followed quickly by a larger increase and then a slower recovery to a value close to the starting size. In the other observed patterns, there is an initial capacitance decrease followed by a slow recovery (Figs. 3 and 5), or a fast capacitance increase with no appreciable initial decrease followed by a faster recovery (Fig 4). The capacitance changes are on the order of 5–20% and more of the initial cell capacitance (Table 2). Except for the variant where capacitance showed only an initial decrease, the average time to complete these capacitance changes was 4.5–5 min. When only the initial capacitance decrease occurs, both the time to reach the maximum change and the time to recover are significantly longer.

Copyright © 2001 by Academic Press. All rights of reproduction in any form reserved.

TABLE 2
Fertilization

	ΔC_m (pF)[a]	ΔC_m %	ΔG_m (nS)	$[Ca^{2+}]_i$ (nM)	Time (min)
Fusion	2.1 ± 0.5 (18)	1.1 ± 0.3	0.3 ± 0.2	No Change (~100)	−2.8 ± 1.5 (Median 3.0)
Activation					
Start ΔC_m				250 ± 130 (11)	0
Start ΔG_m				310 ± 140 (11)	0.1 ± 0.3 (19) (Median 0.1)
Start $\Delta [Ca^{2+}]_i$					−1.4 ± 0.9 (10)
C_m ↓, then ↑, then ↓					
Initial C_m decrease	−9.1 ± 5.3 (14)	−4.7 ± 2.1	1.9 ± 2.8 (Median 0.8)	480 ± 270 (7) (Median 420)	0.3 ± 0.2
Secondary C_m increase	31.5 ± 9.5 (14)	16.8 ± 4.7	11.6 ± 26.9 (Median 3.0)	1060 ± 300 (Median 1010)	0.8 ± 0.5
Recovery C_m	−25.7 ± 8.2 (13)	−13.9 ± 4.1			4.6 ± 2.1
ΔG_m Max			19.0 ± 32.4 (14) (Median 8.3)	1270 ± 580 (Median 1070)	1.9 ± 1.9 (Median 1.1)
Max $[Ca^{2+}]_i$				1420 ± 550 (Median 1090)	1.0 ± 0.5
C_m ↓, then ↑					
Initial C_m decrease	−13.8 ± 8.7 (3)	−7.4 ± 4.0	1.9 ± 0.6	500 ± 90 (3)	1.9 ± 1.3
Recovery C_m	17.0 ± 1.3 (3)	9.5 ± 1.3			13.1 ± 1.2
ΔG_m Max			5.2 ± 2.0 (3)	220 ± 110	5.7 ± 1.6
Max $[Ca^{2+}]_i$				550 ± 60	1.5 ± 0.7
C_m ↑, then ↓					
Initial C_m increase	40.6 ± 19.6 (2)	19.3 ± 8.7	10.9 ± 10.2	3500 (1)	0.2 ± 0.0
Recovery C_m	−65.1 ± 54.3 (2)	−30.7 ± 24.9			4.9 ± 0.2
ΔG_m Max			47.8 ± 54.4 (2)	3100	1.3 ± 0.6
Max $[Ca^{2+}]_i$				5400	0.8
Net ΔC_m	−4.6 ± 14.1 (18) (Median −3.6)	−4.2 ± 12.3 (Median −2.4)			

Note. ΔC_m: Change in membrane capacitance associated with the indicated event; ΔC_m%: Percent ΔC_m vs. the initial capacitance for that cell; ΔG_m: Change in membrane conductance associated with the indicated event; $[Ca^{2+}]_i$: Intracellular free Ca^{2+} concentration at the time of the indicated event; Time: Elapsed time from Start ΔC_m; see text; Start ΔC_m: Inflection point indicating the start of the major capacitance oscillation that follows sperm–egg fusion; Start ΔG_m: Start of the conductance increase that follows activation; Start $\Delta [Ca^{2+}]_i$: Start of the increase in $[Ca^{2+}]_i$ that follows activation; Initial C_m decrease/increase: Values of ΔC_m, ΔG_m, and $[Ca^{2+}]_i$ measured at the first point of maximum change (trough/peak) of the capacitance oscillation. ΔC_m and ΔG_m measured vs. C_m and G_m at Start ΔC_m. Secondary C_m increase: Values of ΔC_m, ΔG_m, and $[Ca^{2+}]_i$ measured at the point of peak capacitance increase following an initial decrease. ΔC_m and ΔG_m measured vs. C_m and G_m at the lowest point of the initial decrease. Recovery: Values of ΔC_m, ΔG_m, and $[Ca^{2+}]_i$ measured at the point capacitance leveled off after the oscillation. ΔC_m and ΔG_m measured vs. C_m and G_m at the lowest/highest point of the initial decrease/increase or from the high point of the secondary increase, as appropriate. ΔG_m Max: Maximum change in membrane conductance measured from G_m at Start ΔG_m. Max $[Ca^{2+}]_i$: $[Ca^{2+}]_i$ at its highest point. Net ΔC_m: Net change in membrane capacitance from Start ΔC_m to Recovery C_m.

[a] Mean ± SD (*n*).

Conductance increases with increased $[Ca^{2+}]_i$. Conductance always increases as a result of egg activation. The increase in conductance is observed solely as inward current (Fig. 1 and data not shown) except for two or three instances of activation by fertilization or with ionophore (see below) when there was a very brief transient of outward current at the beginning of the conductance change. The magnitude of the conductance increase varies greatly, and there is no correlation between the magnitude of this increase and the capacitance change pattern. The peak of the conductance change is usually attained when the capacitance pattern is already in its "recovery" phase. As with capacitance change, the time to reach peak conductance change is slower for the initial capacitance-decrease-only variant than for the other two.

Fertilization-induced changes in $[Ca^{2+}]_i$ in eggs that were patch-clamped consisted of a single major transient with little or no subsequent oscillation in $[Ca^{2+}]_i$. There is a suggestion in the data that the rate and extent of the $[Ca^{2+}]_i$ rise might determine the capacitance change pattern (Table 2): when $[Ca^{2+}]_i$ rose to ~1 μM, the prevalent capacitance oscillation pattern was observed (Fig 2); when $[Ca^{2+}]_i$ rose less vigorously, to ~ 0.5 μM, only an initial capacitance decrease was seen (Figs. 3 and 5). A very vigorous $[Ca^{2+}]_i$

Copyright © 2001 by Academic Press. All rights of reproduction in any form reserved.

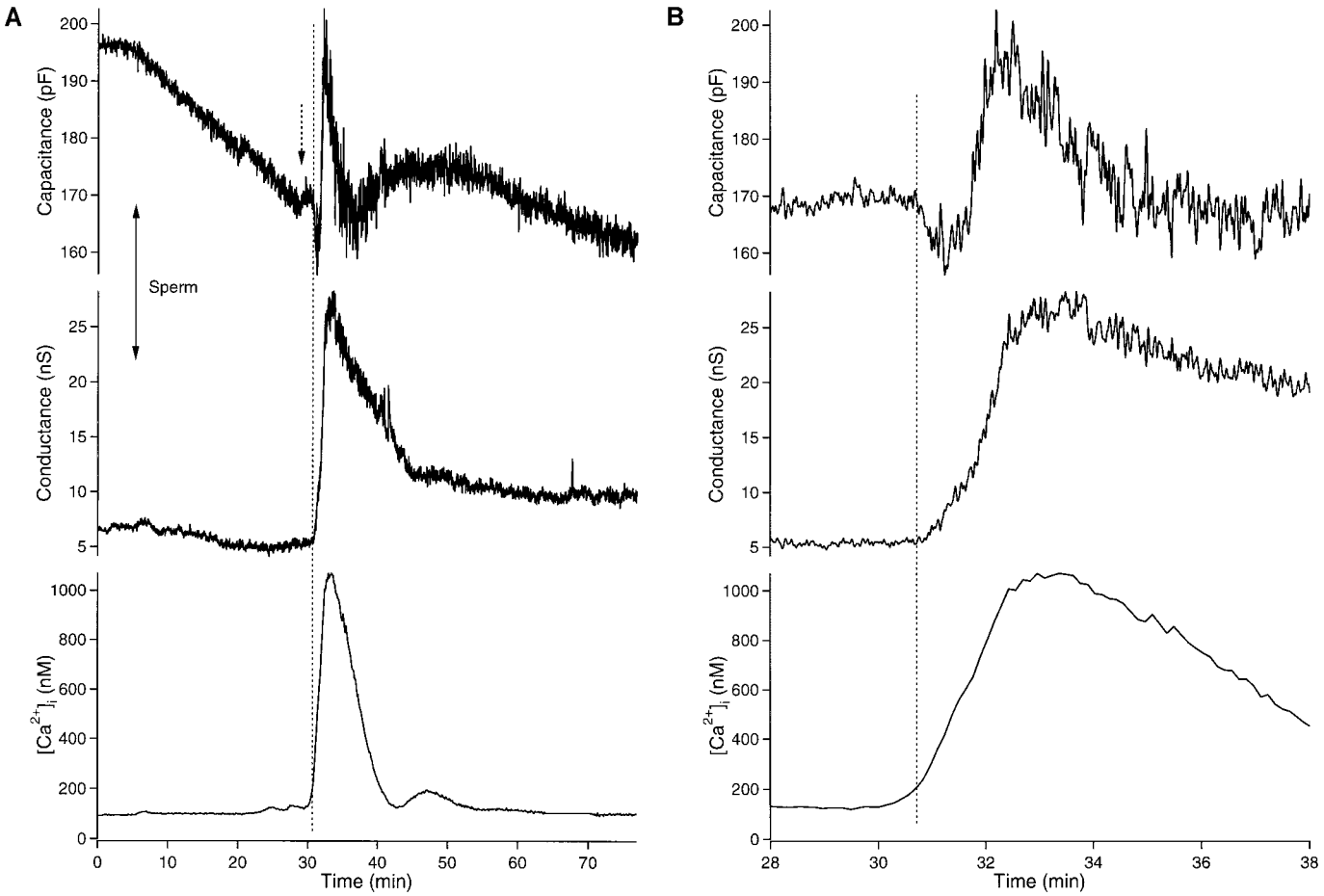

FIG. 2. The most prevalent pattern of sperm-induced changes in membrane capacitance and conductance, correlated with $[Ca^{2+}]_i$. Part A is the entire recording, and part B is the specific period around fertilization. The egg was loaded with fura-2 by incubation with fura-2/AM (see Methods). All other conditions the same as Fig. 1 except that holding potential was −40 mV. A 10-μl sperm suspension was added where indicated.

increase might dictate the capacitance-increase-only pattern (Fig. 4), but we do not have concurrent $[Ca^{2+}]_i$ measurements in other like-behaving cells to support it (see also ionophore data below). For the majority of cells showing a transient capacitance increase, the peak of the $[Ca^{2+}]_i$ increase occurs slightly after the peak capacitance increase; the $[Ca^{2+}]_i$ increase is slightly in advance of capacitance for those cells that only showed the initial capacitance decrease. In almost all instances, the peak conductance was reached when $[Ca^{2+}]_i$ had already begun to fall.

We were able to obtain fertilization in 17 of 38 eggs in whole-cell patch-clamp configuration, but we were concerned that we were perturbing the cells in some fashion by this method. In particular, we found that the Ca^{2+} transients elicited by fertilization in these cells were abnormal in two respects, suggesting changes in Ca^{2+} handling. First, the length of the initial rise in $[Ca^{2+}]_i$ after sperm fusion was longer than expected. Most investigators find that the first Ca^{2+} transient in mouse eggs lasts 2–4 min (e.g., Kline and Kline, 1992). Our own measurements on unpatched fertilizing eggs, some monitored simultaneously with a patched cell, found the length of the first transient to be 3.5 ± 0.9 min (SD, n = 6, median 3.4). However, in patched cells monitored long enough to see the full time course, the Ca^{2+} transient elicited by fertilization lasted 9.5 ± 3.4 min (n = 9, median 8.5). The time for $[Ca^{2+}]_i$ to decline to baseline was much longer, but the time to peak $[Ca^{2+}]_i$ was also longer: 2.4 ± 1.3 min (median 2.2) in patched cells vs 1.1 ± 0.4 min (median 1.1) in the unpatched eggs.

The second difference in patched eggs was that the characteristic Ca^{2+} oscillations that follow the initial $[Ca^{2+}]_i$ increase in fertilized mammalian eggs were inhibited. In eight fertilized eggs monitored for a sufficiently long period after the initial $[Ca^{2+}]_i$ increase, only three showed evidence of additional transients, and these were small and damped out quickly (as in Fig. 2). In contrast, unpatched

Copyright © 2001 by Academic Press. All rights of reproduction in any form reserved.

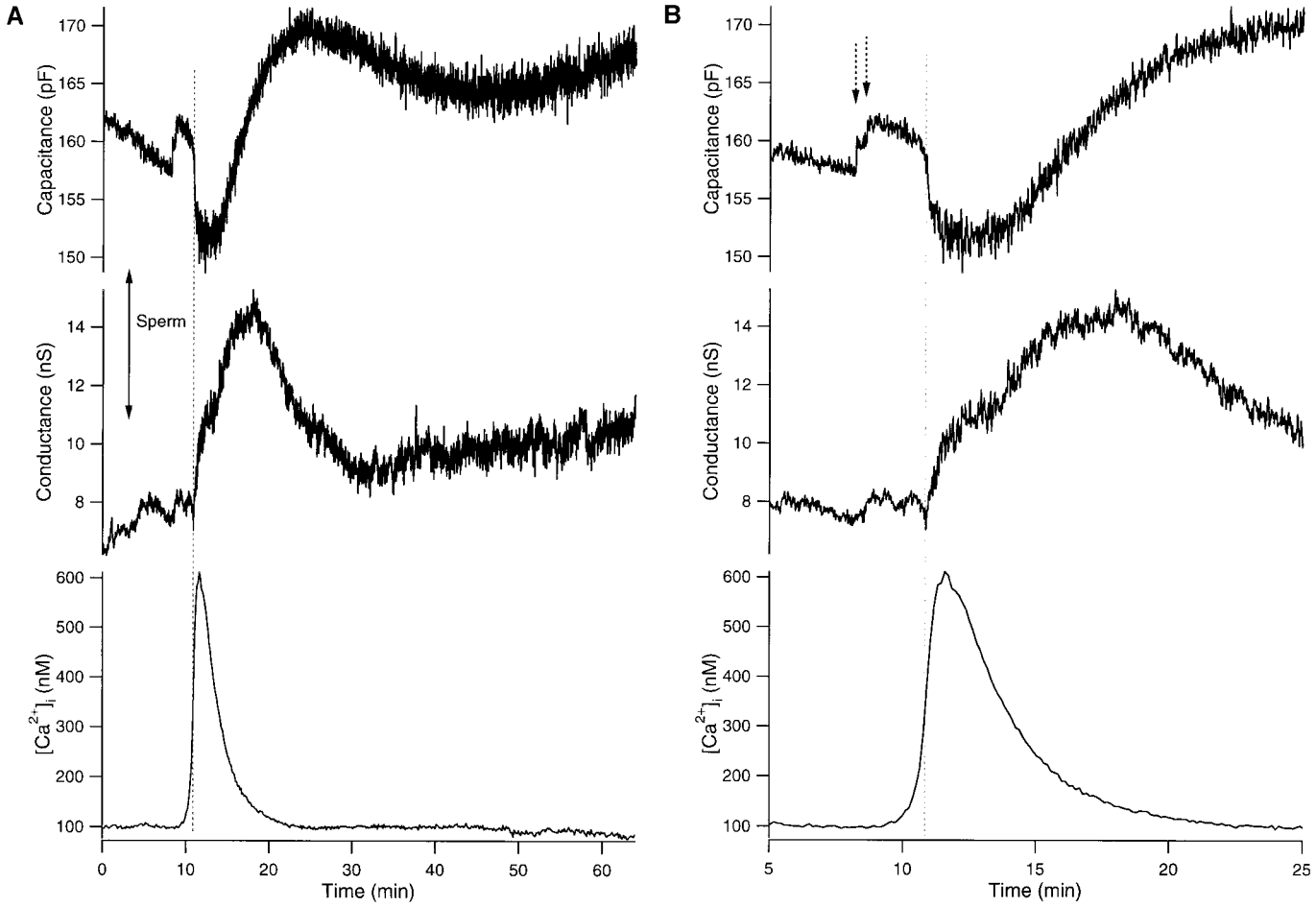

FIG. 3. Primarily capacitance decrease at fertilization. Part A is the entire recording, and part B is the specific period around fertilization. Conditions the same as Fig. 2. This egg was one of four that showed two closely spaced capacitance steps prior to activation.

eggs showed robust secondary Ca^{2+} transients with an average interspike interval of about 15 min. Overall, there is a suggestion that Ca^{2+} handling was perturbed in patch-clamped cells (see also below).

To investigate whether whole-cell configuration was adversely affecting the preparation, we attempted to monitor fertilization with eggs held in perforated-patch configuration. Because intracellular contents are not disturbed to the same extent as in whole-cell mode, perforated patch is generally considered a less invasive method. However, we encountered unexpected difficulties with it. Although the membrane properties of eggs in perforated-patch configuration were equivalent to those in whole-cell mode (Table 1) and tended to be more stable over longer periods of time, only 3 of 24 eggs fertilized in perforated-patch mode. These cells were also different in the amount of time required for fertilization to occur after sperm were added. In whole-cell mode, sperm fusion occurred 13.5 ± 10.5 min after sperm addition (n = 16; median 8.2 min), whereas, in perforated-patch mode, the three fertilizing eggs exhibited sperm fusion only after 48.8 ± 17.6 min (median 39.6 min) in the presence of sperm.

Fig. 5 is one of the three eggs that fertilized in perforated-patch configuration. It shows the same pattern of capacitance, conductance, and $[Ca^{2+}]_i$ change as the whole-cell configuration cell in Fig. 3. The other two fertilizing eggs showed the most common pattern (as in Figs. 1 and 2). However, because of the small number of fertilized eggs and the length of time it took for sperm fusion, we were not able to determine whether the Ca^{2+} handling behavior of these cells was different. Note, though, that the $[Ca^{2+}]_i$ transient in Fig. 5 was still longer than expected.

Sperm Factor-Induced Activation

Cytosolic extracts of mammalian sperm injected into mammalian eggs induce $[Ca^{2+}]_i$ rises very similar to those arising from true fertilization. These $[Ca^{2+}]_i$ rises are neces-

Copyright © 2001 by Academic Press. All rights of reproduction in any form reserved.

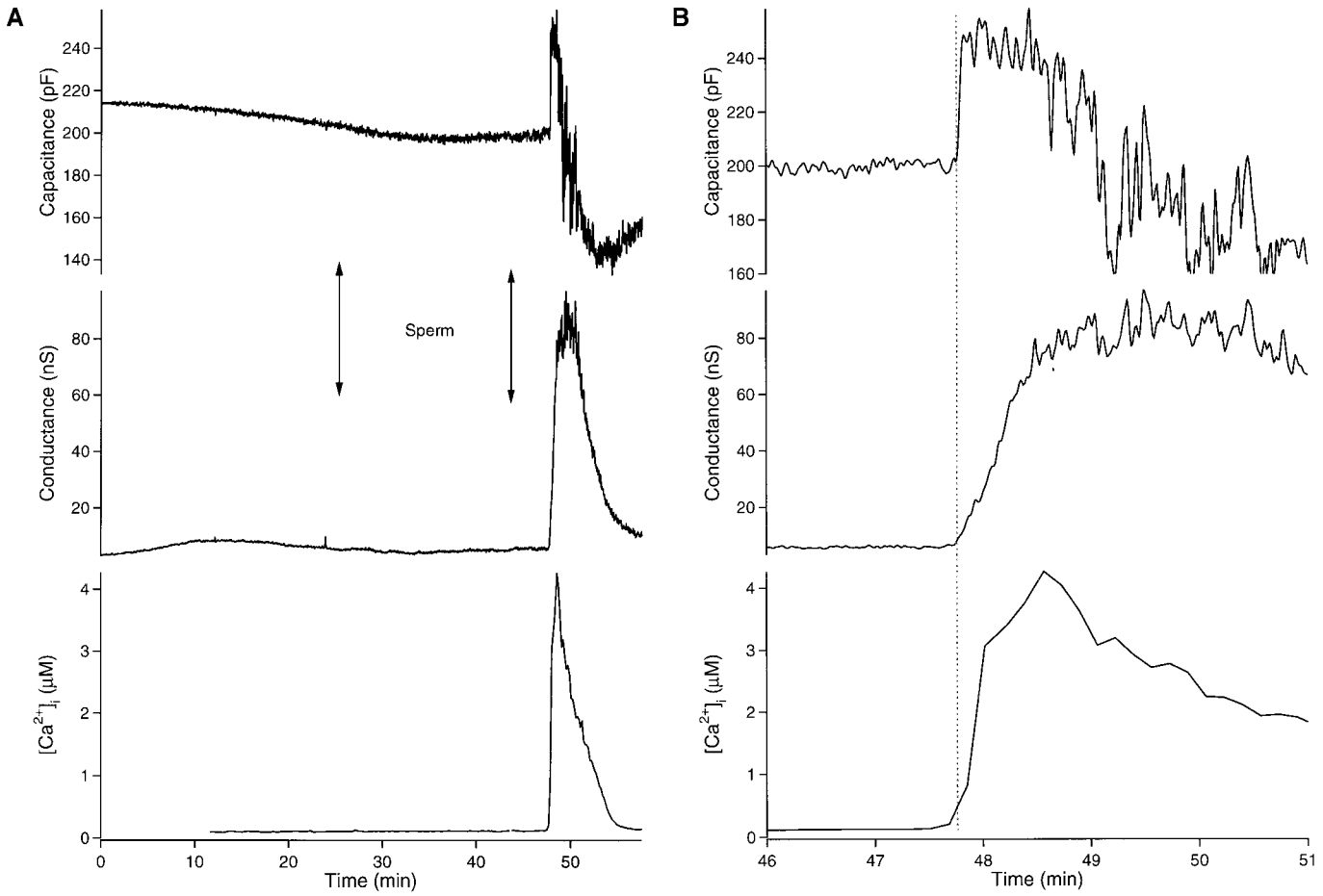

FIG. 4. Primarily capacitance increase at fertilization. Part A is the entire recording, and part B is the specific period around fertilization. This egg was dye-loaded directly from the pipet, which contained the standard fill solution supplemented with 0.26 mM of the potassium salt of fura-2. A 5-μl sperm suspension was added at the first double arrow line, and 10 μl was added at the second. Other conditions the same as Figs. 2 and 3. This was the only egg which showed sperm-induced activation without a clear prior sperm fusion capacitance step.

sary and, perhaps, sufficient to elicit many of the events associated with egg activation (Wu *et al.*, 1998). Sperm factor injected into human eggs was found to activate a Ca^{2+}-dependent K^+ conductance as well as inducing $[Ca^{2+}]_i$ oscillations (Homa and Swann, 1994; Dale *et al.*, 1996).

To determine whether the membrane changes associated with mouse egg fertilization could be mimicked by sperm factor, we performed experiments in which a boar sperm extract was introduced into the cytoplasm of mouse eggs. The extract was placed in the fill solution of the pipet and allowed to diffuse into the interior of a cell in whole-cell patch configuration. It was very difficult to obtain a giga-ohm seal with sperm factor at the tip, so we first placed a small amount of clean fill solution in the tip before back-filling with factor-containing solution. This made for good seals and better recording conditions; but it introduced a variable, sometimes lengthy, delay before intracellular sperm factor reached a concentration sufficient to activate the egg.

Fig. 6 presents two examples of sperm factor-induced egg activation. A slow increase in $[Ca^{2+}]_i$ was initiated from the very beginning of patch rupture, but a characteristic activation capacitance change did not occur until ~20–25 min later when $[Ca^{2+}]_i$ rose to ~250 nM. All 12 eggs treated with sperm factor activated, and most of them exhibited the pattern of the cells in Fig. 6. In these two eggs, as well as on average for sperm-factor activation (Table 3), peak $[Ca^{2+}]_i$ rose to only ~0.5 μM; and the attendant capacitance and conductance changes showed the same relationships and were similar in magnitude to those resulting from similar $[Ca^{2+}]_i$ levels produced by fertilization (Table 2 and Figs. 3 and 5). Changes were slower and more prolonged compared to fertilization, suggesting that the activation threshold was achieved with less than one sperm equivalent of factor. Delays in the time to threshold and rate of $[Ca^{2+}]_i$ increase have been noted before with low concentrations of sperm factor (for example, Oda *et al.*, 1999). We did not find any concentration dependence to the response in the range of

Copyright © 2001 by Academic Press. All rights of reproduction in any form reserved.

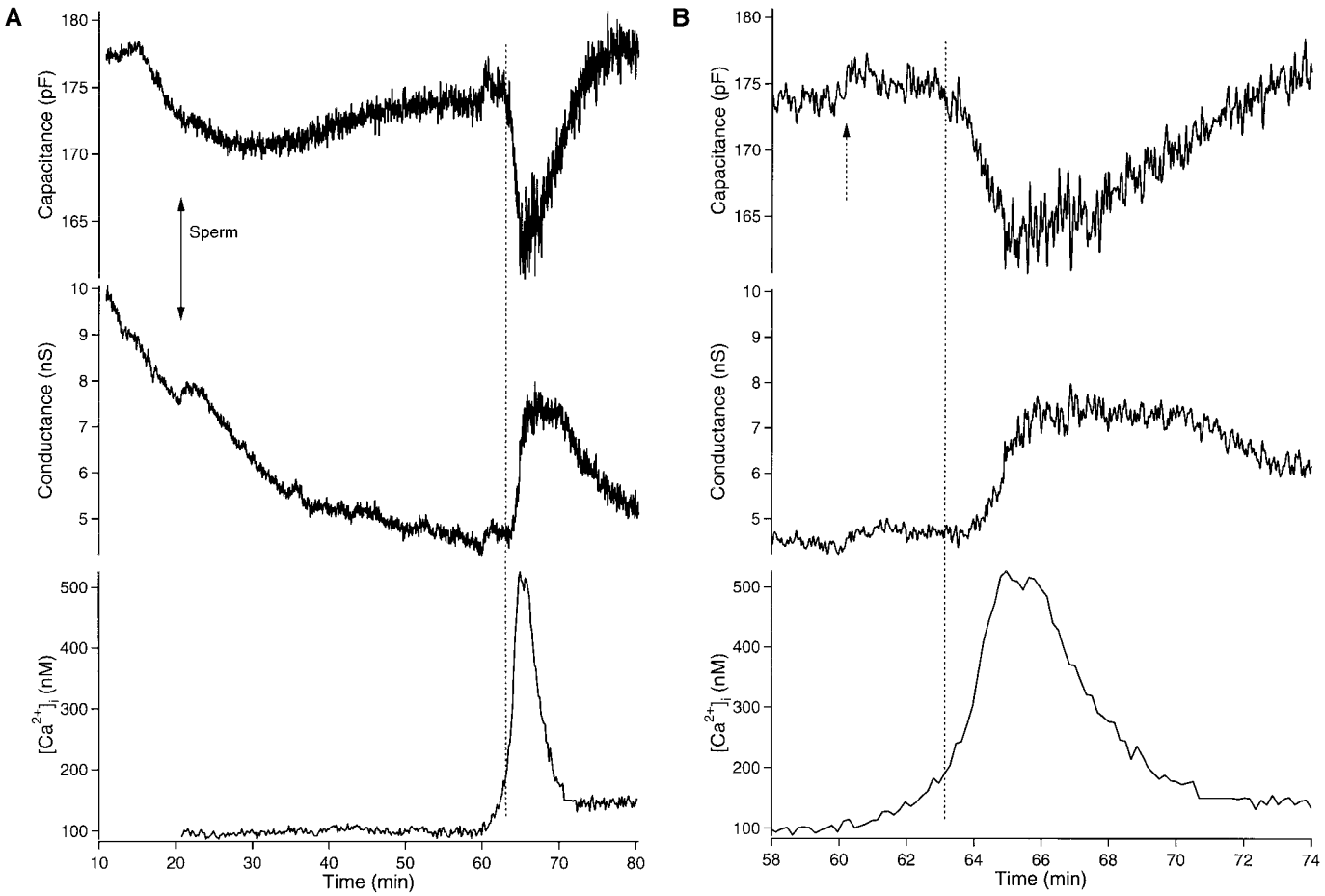

FIG. 5. Fertilization of an egg in perforated-patch configuration. Part A is the entire recording, and part B is the specific period around fertilization. Zero time is from the point of seal formation and the initiation of patch permeabilization. The bath solution was the simple saline (see Methods), and the pipet fill solution was supplemented with 200 μg/ml Pluronic F-127 and 250 μg/ml nystatin (see Methods). Other conditions the same as Figs. 2 and 3.

1–3 μg/μl final pipet concentration. With sperm factor infusion, we never observed the earlier 2-pF capacitance step that we take to be indicative of sperm fusion.

Repetitive $[Ca^{2+}]_i$ transients are a feature of sperm factor-induced activation, as they are of normal fertilization (e.g., Oda *et al.*, 1999). In recordings maintained for a sufficiently long time, we observed secondary $[Ca^{2+}]_i$ transients in 6 of 10 eggs activated by sperm factor perfusion. However, as in the fertilized eggs described above, these $[Ca^{2+}]_i$ transients were almost invariably small and damped out quickly. The second $[Ca^{2+}]_i$ transient in the egg in Fig. 6B was the largest we observed in any patch-clamped cell, and the only one to have a clear effect on capacitance and conductance.

Forced $[Ca^{2+}]_i$ Rise: Ionophore

It is generally observed that many aspects of early egg activation and development can be mimicked by raising $[Ca^{2+}]_i$ with Ca^{2+} ionophore (e.g., Kline and Kline, 1992). To look at the role of $[Ca^{2+}]_i$ in fertilization-induced membrane changes, we investigated the effect of adding a bolus of ionomycin-containing saline to whole-cell patch-clamped mouse eggs. This proved to be a difficult undertaking, as even very small amounts of ionomycin could lead to an unpredictable, explosive increase in $[Ca^{2+}]_i$ that was deleterious to the recording and/or the cell. In those eggs with a more favorable response, we observed the same three patterns of capacitance change seen previously with fertilized eggs (Table 4). Within the considerable scatter of these measurements, there was no meaningful difference in the size of capacitance changes induced by fertilization or ionophore. The pace of changes may have been slower in ionophore-activated eggs that followed the standard pattern, but these rates were the same as in fertilized eggs for those that showed only initial capacitance increase or decrease. $[Ca^{2+}]_i$ reached very high levels in standard-pattern,

Copyright © 2001 by Academic Press. All rights of reproduction in any form reserved.

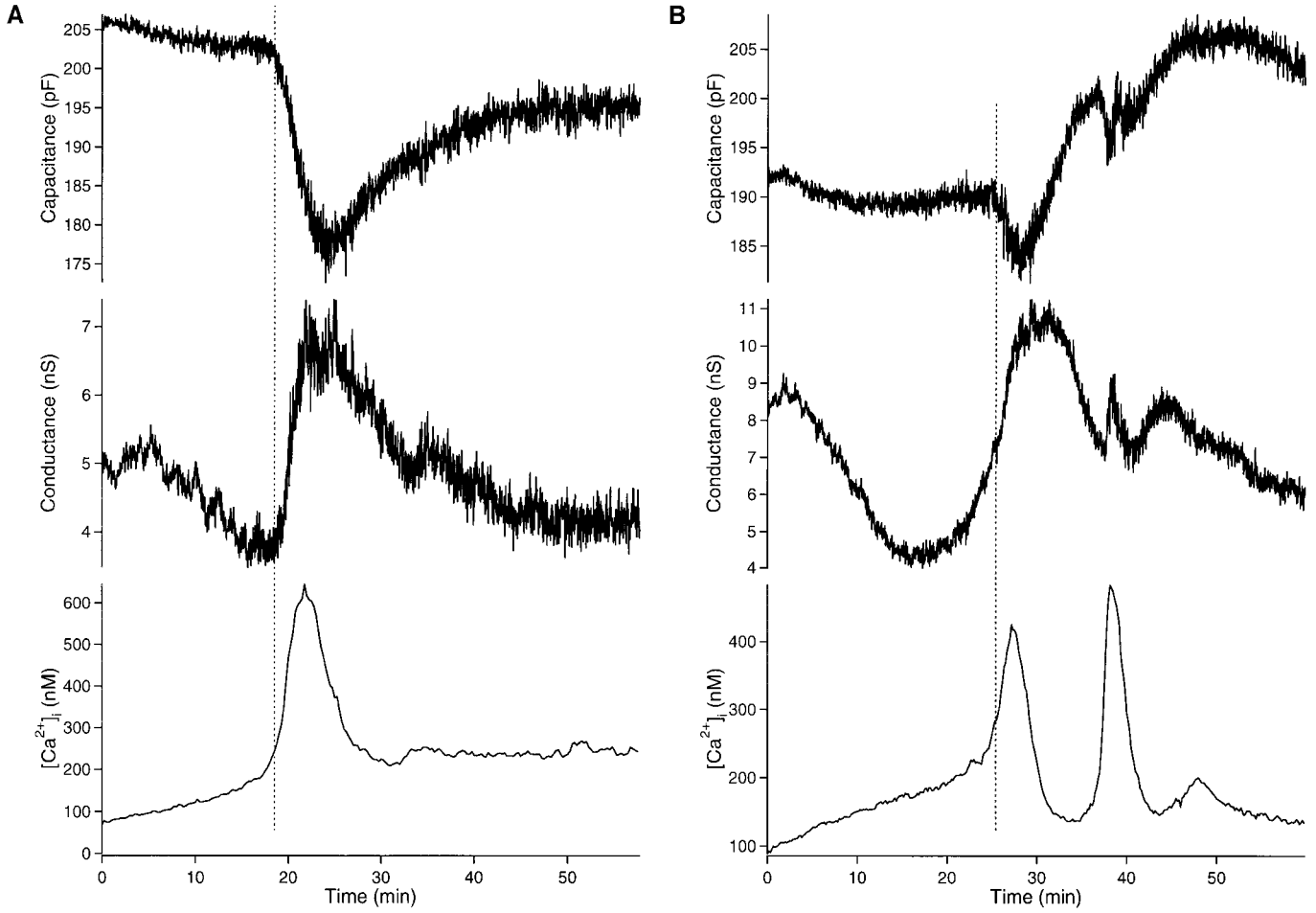

FIG. 6. Egg changes induced by infusion of sperm factor. Eggs were preloaded with fura-2/AM and then placed into whole-cell patch configuration. Zero time is from patch rupture. The fill solution was the standard formulation supplemented to 10% (A) or 15% (B) sperm factor from a 10 μg/μl stock. Bath solution was the simple saline for both cells. Other conditions the same as Figs. 2 and 3.

ionophore-activated eggs, but it took much longer than in fertilized eggs to come to the final peak value. An example of such ionophore-driven changes is shown in Fig. 7.

The incidence of eggs showing only an initial capacitance increase was higher with ionophore than with fertilization (5/12 vs 2/19; Tables 2 and 4), but we do not have concurrent Ca^{2+} imaging data with these cells to see if this reflected a faster and/or larger ionophore-induced increase in $[Ca^{2+}]_i$. Although capacitance and conductance changes occurred quickly in these cells, we had trouble holding them to recovery (Table 4), suggesting the possibility of an overwhelming Ca^{2+} load.

Forced $[Ca^{2+}]_i$ Rise: IP_3

Considerable evidence indicates that the rise in $[Ca^{2+}]_i$ at mammalian egg fertilization is due to IP_3-mediated release of intracellular Ca^{2+} stores (Miyazaki *et al.*, 1993). The egg-activating component of sperm factor may be an unusual, sperm-specific soluble phospholipase C (Jones *et al.*, 2000). To test whether IP_3-induced $[Ca^{2+}]_i$ increase would initiate the same membrane changes as fertilization and ionophore, we performed experiments with IP_3 in the pipet fill solution. Our pipets were filled to the tip with IP_3-containing solution, so effects occurred quickly after patch rupture.

With a low concentration of IP_3 in the pipet (1 μM), $[Ca^{2+}]_i$ showed a modest, prolonged increase (estimated rise to ~200 nM), and there were no capacitance or conductance changes. With higher IP_3 concentrations ($\geq$10 μM), $[Ca^{2+}]_i$ rose quickly and elicited the same types of capacitance change patterns observed for fertilization and ionophore. Fig. 8 shows an example of typical IP_3-induced changes. Again, a capacitance increase was most likely when $[Ca^{2+}]_i$ went to high levels ($>$ 1μM), and an initial capacitance decrease was favored when $[Ca^{2+}]_i$ remained lower (Table 5).

Copyright © 2001 by Academic Press. All rights of reproduction in any form reserved.

TABLE 3
Sperm Factor

	ΔC_m (pF)[a]	ΔC_m %	ΔG_m (nS)	$[Ca^{2+}]_i$ (nM)	Time (min)
C_m ↓, then ↑					
Start ΔC_m				260 ± 50 (11) (Median 250)	0
Start ΔG_m				330 ± 150 (11) (Median 310)	1.1 ± 2.9 (Median 0.7)
Start $\Delta [Ca^{2+}]_i$					−2.9 ± 1.5 (Median −2.5)
Initial C_m decrease	−23.1 ± 19.4 (11) (Median −25.0)	−11.4 ± 8.8 (Median −12.2)	1.6 ± 2.4 (Median 1.1)	400 ± 140 (Median 410)	6.0 ± 4.3 (Median 5.3)
Recovery C_m	19.8 ± 7.2 (7) (Median 17.9)	10.9 ± 6.5 (Median 9.1)			21.5 ± 12.0 (Median 16.2)
ΔG_m Max			4.2 ± 2.7 (10) (Median 3.7)	410 ± 160 (Median 410)	5.8 ± 3.4 (Median 4.8)
Max $[Ca^{2+}]_i$				550 ± 280 (Median 440)	3.9 ± 2.3 (Median 3.2)
C_m ↑, then ↓					
Start ΔC_m				170 (1)	0
Start ΔG_m				100	−0.6
Start $\Delta [Ca^{2+}]_i$					−0.9
Initial C_m increase	21.3 (1)	15.7	19.3	320	1.1
Recovery C_m	−66.3	−48.8			13.4
ΔG_m Max			22.2	430	1.4
Max $[Ca^{2+}]_i$				870	4.1
C_m ↓, then ↑, then ↓					
None					
Net ΔC_m	−5.1 ± 26.8 (8) (Median 1.0)	−2.5 ± 16.9 (Median 0.4)			

[a] Mean ± SD (*n*).

Previous studies have found that repetitive $[Ca^{2+}]_i$ transients can be elicited in mammalian eggs by IP_3 introduced by injection (Kline and Kline, 1994) or by continuous diffusion from an injection needle (Swann, 1992). In our experiments, the IP_3-induced $[Ca^{2+}]_i$ increase was transient and occurred only the one time, even though the cell interior was subject to a continuous infusion of IP_3. Even when we tried to mimic an "IP_3 injection" by going into whole-cell configuration with IP_3 in the pipet and then pulling off the pipet during the resultant $[Ca^{2+}]_i$ increase, there were no additional $[Ca^{2+}]_i$ transients ($n = 3$).

Under our conditions, $[Ca^{2+}]_i$ did not return to the initial value after the transient but remained at ~200 nM (Figs. 8 and 9). This appears to be the result of continuous infusion of IP_3; when the IP_3-containing pipet was pulled off the cell, $[Ca^{2+}]_i$ returned to resting levels in ~5 min. With a high concentration of IP_3 in the cytoplasm, the stores should not be able to refill.

Although IP3-induced capacitance changes were similar to those produced by fertilization and showed a similar correlation with $[Ca^{2+}]_i$, IP_3-induced conductance changes were different (Fig. 8). Even when $[Ca^{2+}]_i$ went very high, the increase in conductance was generally slow to develop and quite prolonged. The only fertilized eggs that behaved similarly were those that showed only an initial capacitance decrease (Tables 2 and 5).

To learn something of the nature of this conductance, we performed a slightly different type of experiment. Instead of imposing repetitive voltage steps to monitor capacitance and membrane resistance, we utilized a series of voltage ramps that could give us directly the conductance (from the slope) and the zero current potential. Fig. 9 is one of five such experiments that gave essentially identical results. An initial depolarization of a few mV was associated with a very minor change in conductance. Subsequently, the magnitude of the conductance approximately doubled with little or no change in the reversal potential. This indicates that the reversal potential of the current(s) activated during this conductance increase is similar to the initial membrane potential and is in the region of −35 mV. In contrast, the membrane potential changes produced by ionophore in three similar voltage ramp experiments were strongly depolarizing (data not shown).

Forced $[Ca^{2+}]_i$ Rise: I_{Ca}

Mouse eggs have a T-type voltage-gated Ca^{2+} channel (I_{Ca}) of unknown function (Peres, 1987; Day *et al.*, 1998). If the

Copyright © 2001 by Academic Press. All rights of reproduction in any form reserved.

TABLE 4
Ionomycin

	ΔC_m (pF)[a]	ΔC_m %	ΔG_m (nS)	$[Ca^{2+}]_i$ (nM)	Time (min)
Activation					
Start ΔC_m				410 ± 300 (5) (Median 250)	0
Start ΔG_m				1170 ± 930 (5) (Median 900)	0.3 ± 0.2 (12) (Median 0.2)
Start $\Delta [Ca^{2+}]_i$					−0.7 ± 0.7 (5) (Median −0.4)
C_m ↓, then ↑, then ↓					
Initial C_m decrease	−6.8 ± 4.3 (5) (Median −6.1)	−3.9 ± 1.9	0.6 ± 0.7 (Median 0.4)	570 ± 430 (4) (Median 420)	0.7 ± 0.8 (Median 0.6)
Secondary C_m increase	20.6 ± 9.4 (5)	12.3 ± 4.9	7.8 ± 11.9 (Median 3.9)	1240 ± 420 (Median 1160)	2.3 ± 2.6 (Median 1.6)
Recovery C_m	−17.5 ± 6.3 (5)	−10.3 ± 2.1			6.2 ± 5.3 (Median 4.7)
ΔG_m Max			28.8 ± 35.5 (5) (Median 9.4)	3100 ± 2800 (Median 2400)	2.7 ± 2.4 (Median 1.7)
Max $[Ca^{2+}]_i$				4900 ± 2500 (Median 5700)	4.4 ± 4.8 (Median 2.9)
C_m ↓, then ↑					
Initial C_m decrease	−21.8 ± 16.5 (2)	−12.0 ± 8.6	3.5 ± 1.5	780 (1)	1.7 ± 0.8
Recovery C_m	16.9 ± 3.9 (2)	9.4 ± 1.7			12.1 ± 3.7
ΔG_m Max			10.3 ± 6.6 (2)	500	5.4 ± 3.3
Max $[Ca^{2+}]_i$				950	0.5
C_m ↑, then ↓					
Initial C_m increase	15.1 ± 7.1 (5)	10.9 ± 5.0	2.5 ± 2.5 (Median 1.3)		0.2 ± 0.1
Recovery C_m	−13.0 ± 3.9 (3)	−9.1 ± 2.7			2.0 ± 1.9 (Median 1.2)
ΔG_m Max			12.2 ± 8.3 (5)		1.9 ± 1.9 (Median 1.1)
Max $[Ca^{2+}]_i$					
Net ΔC_m	−3.1 ± 11.5 (10) (Median −1.3)	−1.7 ± 6.4 (Median −1.3)			

[a] Mean ± SD (*n*).

membrane changes we observe at fertilization are truly a consequence of the rise in $[Ca^{2+}]_i$, then it would be valuable to determine the effect of Ca^{2+} brought into the egg by activation of I_{Ca}.

At our normal holding potential (−40 mV), I_{Ca} is completely inactivated and does not enter into any of our measurements. The current trace in response to a voltage ramp from −50 to +20 mV as used in Fig. 9 is almost perfectly linear (Fig. 9 inset). Inactivation of I_{Ca} is relieved at considerably more hyperpolarized membrane potentials (Peres, 1987). From a holding potential of −80 mV, we found maximal activation of this current with depolarization to −20 or −30 mV. However, the current inactivates completely in 40–50 ms with sustained depolarization (Fig. 10A inset), and there is no measurable increase in $[Ca^{2+}]_i$ produced by a single voltage step. To bring in the maximum amount of Ca^{2+}, we applied trains of quickly repetitive pulses. The protocol that we used most was 20-ms steps applied every 100 ms, which did not fully inactivate the current during the step and allowed for near complete recovery before applying the next one.

Fig. 10 is an example of an egg treated in this way. We were able to drive bulk egg $[Ca^{2+}]_i$ to ~600 nM and cortical $[Ca^{2+}]_i$ to ~900 nM with a series of pulse trains (Fig. 10B). This rise in $[Ca^{2+}]_i$ initiated a substantial decrease in capacitance and a small increase in conductance. Once a plateau capacitance level was attained, further increases in $[Ca^{2+}]_i$ had no effect (Fig. 10A). At no time were we able to stimulate an increase in capacitance by activation of I_{Ca}.

This change in capacitance initiated by raising $[Ca^{2+}]_i$ with I_{Ca} was slower than that produced by the other egg-activating agents. Since we saw occasional inflections in the capacitance drift of unstimulated cells, we quantitated the maximal rate of capacitance change in resting vs I_{Ca}-stimulated eggs. In whole-cell patch-clamped cells, the average maximal rate of capacitance decrease was 1.0 ± 0.7

Copyright © 2001 by Academic Press. All rights of reproduction in any form reserved.

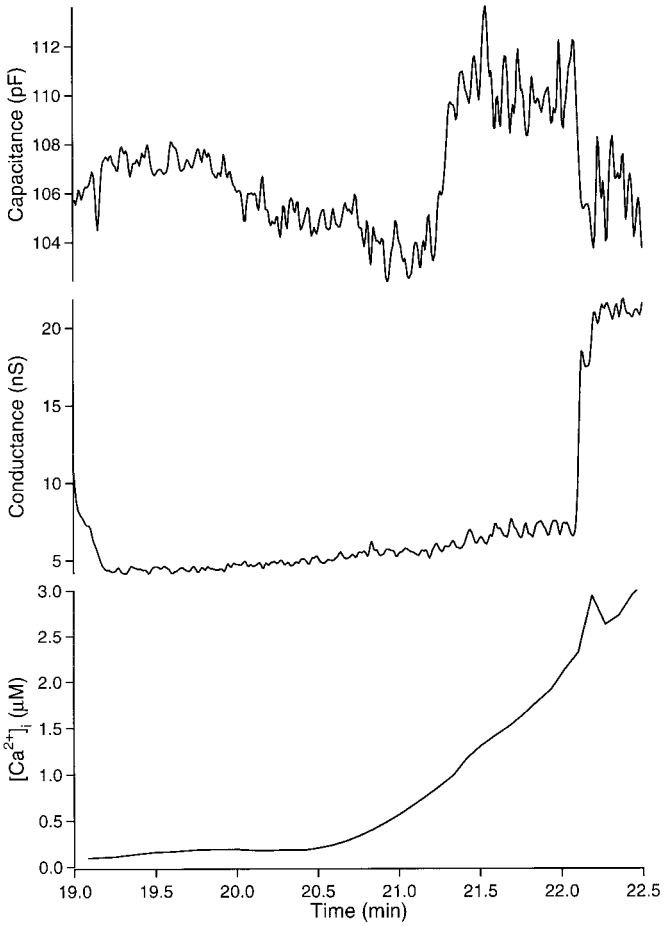

FIG. 7. Forced $[Ca^{2+}]_i$ rise with Ca ionophore. Egg was preloaded with fura-2/AM and placed into whole-cell patch configuration. Bath was M2 Ringer, and pipet fill solution was the standard formulation. A bolus of 5 μl of 20 μM ionomycin was added at some distance from the cell just before the start of this record. Both $[Ca^{2+}]_i$ and conductance continued to increase after the period shown. The earlier part of this recording was given to looking at the effect of activating I_{Ca}, but this had been ineffective and had led to no changes in conductance or capacitance. Holding potential during ionomycin addition was −80 mV.

pF/min (n = 53, median 1.0). A few eggs showed drift to larger capacitance, and eggs in perforated-patch configuration had smaller maximal rates. In the four whole-cell clamped eggs that showed an apparent induced capacitance decrease in response to I_{Ca} pulse trains, the maximal rate of capacitance decrease was 4.2 ± 1.6 pF/min (median 4.2), and the rate in three of four cells was greater than the largest value observed in any resting cell.

The increase in conductance in response to I_{Ca} pulse trains was not significant in all experiments and may in part arise from general cellular stress when the membrane is clamped at −80 mV. As can be seen in Fig. 10A, the noisiness of the records increases at −80 mV and there are conductance changes associated simply with the change from −40 to −80 mV and back.

DISCUSSION

Fertilization

Sperm fusion is indicated by an ~2-pF step increase in mouse egg capacitance and an ~0.3-nS increase in conductance. We did not have another physical assay of sperm–egg fusion, but this characteristic change in capacitance did not occur with any other method of activation. $[Ca^{2+}]_i$ is stable during sperm–egg fusion, and there are no observed changes in egg electrophysiological parameters or $[Ca^{2+}]_i$ as a result of sperm binding prior to fusion, even as they are flailing away vigorously on the egg surface.

After the fusion event itself, the earliest consequence of egg activation was an accelerating increase in $[Ca^{2+}]_i$ that began ~1 min after sperm fusion. About 1.5 min after $[Ca^{2+}]_i$ began to rise, a threshold $[Ca^{2+}]$ (averaged over the center of the egg) of ~250 nM was reached that initiated a change in capacitance. A conductance increase was usually observed when $[Ca^{2+}]$ reached ~300 nM. Activating protocols that raised $[Ca^{2+}]_i$ but did not reach this threshold (e.g., I_{Ca} or low $[IP_3]$) did not initiate capacitance change.

All $[Ca^{2+}]_i$ values that we report are based on in vitro calibration and an assumed K_d. As such, they should be considered estimates. Nevertheless, the trends observed and the apparent $[Ca^{2+}]_i$ values at which electrophysiological events occurred were reproducible. Even if the values are off by some factor, the relationships among them during the various phases of the response should remain valid.

Although measured $[Ca^{2+}]_i$ values were very consistent, they were determined from the central part of the egg. Our experimental setup did not allow us to simultaneously observe the sperm in bright field along with the fluorescent signal from the calcium indicator in the egg, so we were unable to identify and monitor the region of sperm–egg fusion. Deguchi *et al.* (2000) have done this with higher resolution equipment and found that $[Ca^{2+}]$ at the sperm fusion site increases a few seconds earlier than other areas of the egg. Moreover, intracellular Ca^{2+} released at fertilization is derived from endoplasmic reticulum concentrated under the egg cortex (Kline *et al.*, 1999). Hence, $[Ca^{2+}]_i$ is likely to be higher in the subcortical region where exocytosis and endocytosis are controlled. In the instance where we were using I_{Ca} to bring Ca^{2+} directly into the subcortical region (Fig. 10), we observed peripheral $[Ca^{2+}]_i$ to be ~50% higher than that measured in the center. Even this difference is probably an underestimate, because our peripheral $[Ca^{2+}]_i$ measurement is still not specific to the region just under the cortex. This suggests that efficacious $[Ca^{2+}]_i$ levels are likely to be higher than we report based on our bulk cytoplasmic measurements.

In the majority of cells, the initial capacitance change was a decrease. This was usually followed quickly by a larger capacitance increase. But, in cells where peak $[Ca^{2+}]_i$

Copyright © 2001 by Academic Press. All rights of reproduction in any form reserved.

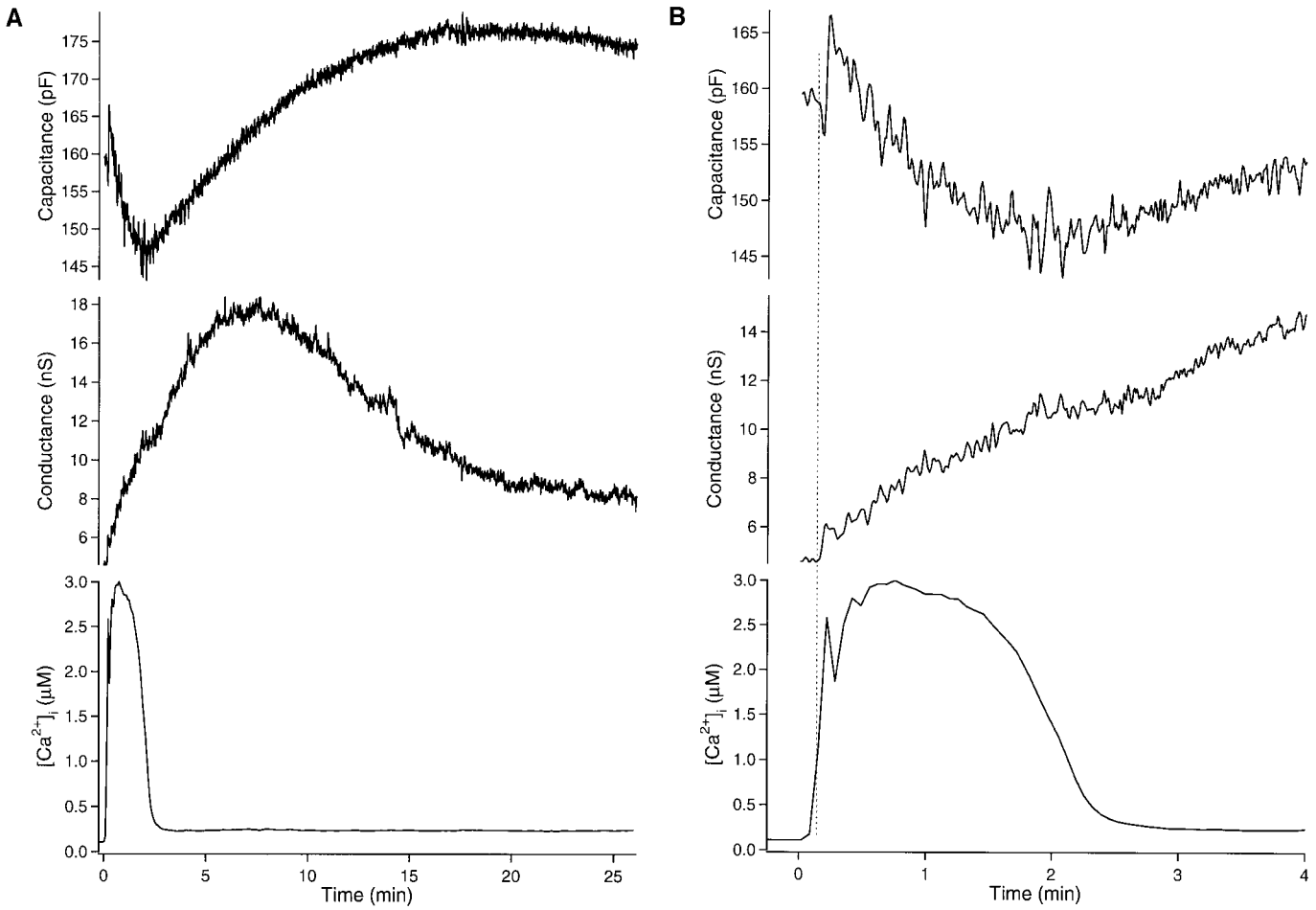

FIG. 8. Forced $[Ca^{2+}]_i$ rise with IP_3. Part A is the entire recording, and part B is the specific period around the peak of the IP_3 response. Egg was preloaded with fura-2/AM and placed into whole-cell patch configuration. Membrane parameters and $[Ca^{2+}]_i$ were monitored during patch rupture. The standard pipet solution was supplemented with 30 μM IP_3. Bath was M2 Ringer. Holding potential was −40 mV.

was sub-μM, a capacitance decrease was usually the dominant effect. The expectation was that egg activation would lead to an immediate increase in membrane surface area due to secretion of the cortical granules, followed by a gradual decline to about the original surface area as newly inserted membrane was recovered. This was the pattern observed in hamster eggs (Kline and Stewart-Savage, 1994). But capacitance can only report net changes, and it is very likely that exocytosis and endocytosis are occurring together whenever vesicular secretion is stimulated. Nevertheless, the prominence of early capacitance decreases here was somewhat surprising.

Our data from fertilization and the other manipulations that raised $[Ca^{2+}]_i$ suggest that both endocytosis and exocytosis are Ca^{2+}-driven in the mouse egg, and that endocytosis may be more sensitive to $[Ca^{2+}]$ and/or have a lower threshold. Any increase in $[Ca^{2+}]_i$ above ~250 nM initiated a capacitance change, and this change was primarily an increase only when $[Ca^{2+}]_i$ rose very high very quickly (Fig. 4). When $[Ca^{2+}]_i$ rose to a high level (>1 μM) but did so more slowly, capacitance increased only after an initial transient decrease (Fig. 2), suggesting that net endocytosis stimulated at low $[Ca^{2+}]_i$ was converted to net exocytosis when $[Ca^{2+}]_i$ went higher. When $[Ca^{2+}]_i$ rose only to ~500 nM, then a longer and larger initial capacitance decrease occurred (Figs. 3, 5, 6, and 10), suggesting that exocytosis received a weaker stimulus under these conditions. Using a dye-based method, Tahara *et al.* (1996) showed that fertilization-induced membrane turnover continues for 45–60 min in the mouse egg. The interpretation of their data requires long-term stimulation of both exocytosis and endocytosis, although they would be unable to detect endocytosis separate from exocytosis. We cannot say to what extent, if any, exocytosis and endocytosis were uncoupled in our observations. We might be able to address this by combining electrophysiological measurements with monitoring of a

Copyright © 2001 by Academic Press. All rights of reproduction in any form reserved.

TABLE 5
IP_3

	ΔC_m (pF)[a]	ΔC_m %	ΔG_m (nS)	$[Ca^{2+}]_i$ (nM)	Time (min)
C_m ↓, then ↑, then ↓					
Start ΔC_m				510 ± 350 (3) (Median 410)	0
Start ΔG_m				1060 ± 190 (2)	0.03 ± 0.03
Start $\Delta [Ca^{2+}]_i$					−0.27 ± 0.20 (3) (Median −0.16)
Initial C_m decrease	−3.1 ± 0.5 (3) (Median −3.0)	−2.2 ± 0.5 (Median −1.9)	1.6 ± 1.3 (Median 0.9)	1190 ± 570 (Median 1090)	0.07 ± 0.03 (Median 0.06)
Secondary C_m increase	13.3 ± 2.3 (Median 13.7)	8.8 ± 1.8 (Median 9.8)	1.7 ± 1.2 (Median 2.3)	1410 ± 820 (Median 1230)	0.30 ± 0.34 (Median 0.13)
Recovery C_m	−16.9 ± 3.5 (2)	−10.8 ± 2.0			1.76 ± 0.04
ΔG_m Max			21.9 ± 15.9 (3) (Median 13.6)	190 ± 50 (Median 200)	7.7 ± 1.7 (Median 7.4)
Max $[Ca^{2+}]_i$				1880 ± 940 (Median 1420)	0.40 ± 0.27 (Median 0.50)
C_m ↓, then ↑					
Start ΔC_m				370 ± 130 (6) (Median 350)	0
Start ΔG_m				630 ± 260 (4) (Median 550)	0.5 ± 0.4 (Median 0.5)
Start $\Delta [Ca^{2+}]_i$					−0.8 ± 0.6 (Median −0.6)
Initial C_m decrease	−11.4 ± 7.5 (6) (Median −9.0)	−5.9 ± 3.3 (Median −5.2)	2.3 ± 2.5 (Median 1.4)	370 ± 120 (Median 350)	1.5 ± 0.7 (Median 1.6)
Recovery C_m	26.1 ± 2.5 (2)	14.7 ± 3.2			14.2 ± 0.7
ΔG_m Max			10.2 ± 3.2 (3) (Median 8.6)	240 ± 60 (Median 210)	8.8 ± 2.4 (Median 8.2)
Max $[Ca^{2+}]_i$				620 ± 230 (Median 610)	0.6 ± 0.3 (Median 0.6)
C_m ↑, then ↓					
None					
Net ΔC_m	2.0 ± 13.6 (4) (Median −0.7)	1.1 ± 8.4 (Median −0.5)			

[a] Mean ± SD (*n*).

membrane-marker dye as per Tahara *et al.* (1996) and/or testing for release of cortical granule contents.

Sperm Factor Is Similar to Fertilization

Introducing porcine sperm factor into the egg by diffusion from the patch pipet led to the same electrophysiological changes that characterized fertilization. Moreover, these changes appeared to be tied to $[Ca^{2+}]_i$ in the same way, as capacitance and conductance changes initiated at the same $[Ca^{2+}]_i$ as in fertilized eggs. We mostly observed the pattern where capacitance exhibited only an initial decrease, but this was consistent with our observation among fertilized eggs that sub-μM peak $[Ca^{2+}]_i$ favored this pattern. Since sperm factor is an extract of the cytosolic part of the sperm, these results suggest that the sperm membrane does not contribute significantly to the electrophysiological changes seen in the mouse egg after sperm fusion.

The Effect of IP_3 on Capacitance and Conductance Is a Little Different

The direct introduction of IP_3 from the patch pipet led to a very rapid rise in $[Ca^{2+}]_i$ and the prompt initiation of capacitance change. The pattern of capacitance change still correlated with peak $[Ca^{2+}]_i$ in the same way as noted for fertilization and sperm-factor activation. The apparent threshold for activation of capacitance change was higher for IP_3, but this could be an artifact of the fast rise of the IP_3-induced $[Ca^{2+}]_i$ increase and our relatively poor time resolution on the Ca^{2+} measurement. Alternatively, there may be a short delay in the initiation of the capacitance change after threshold that makes it appear to be less

Copyright © 2001 by Academic Press. All rights of reproduction in any form reserved.

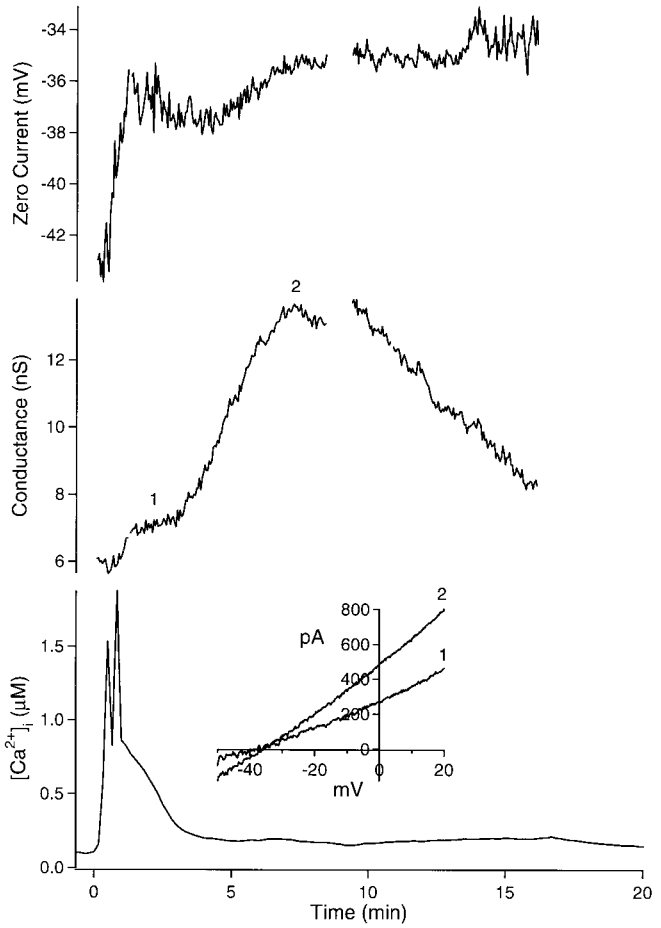

FIG. 9. Voltage ramps during forced $[Ca^{2+}]_i$ rise with IP_3. Egg was preloaded with fura-2/AM and placed into whole-cell patch configuration. $[Ca^{2+}]_i$ was monitored during patch rupture, and voltage ramps were initiated just after. Voltage ramps from −50 to +20 mV were applied every 3 s. The representative numbered traces on the inset correspond to the same numbered points on the analyzed data trace. Membrane potential was held at −40 mV between ramps. Gaps in the recording are periods when the voltage ramps were stopped to check access resistance. Conductance was determined from the slope of a least squares linear fit to the current trace between −45 and +10 mV. Zero current potential was calculated from the linear fit. The pipet contained the standard fill solution supplemented with 20 μM IP_3 without MgATP. Bath was the simple saline.

sensitive when the $[Ca^{2+}]_i$ increase was produced in this way.

The most striking difference observed as a result of IP_3-induced activation was the slow onset and prolonged time course of the conductance increase. Although there was usually some increase in conductance shortly after the initiation of the capacitance change, it was almost always very modest at first. And the full conductance increase took longer to develop than in fertilized or sperm factor-activated eggs, even though the $[Ca^{2+}]_i$ transient in IP_3-activated eggs was more vigorous and decayed more quickly. This raises the possibility that sperm and sperm factor do more than initiate a rise in $[Ca^{2+}]_i$.

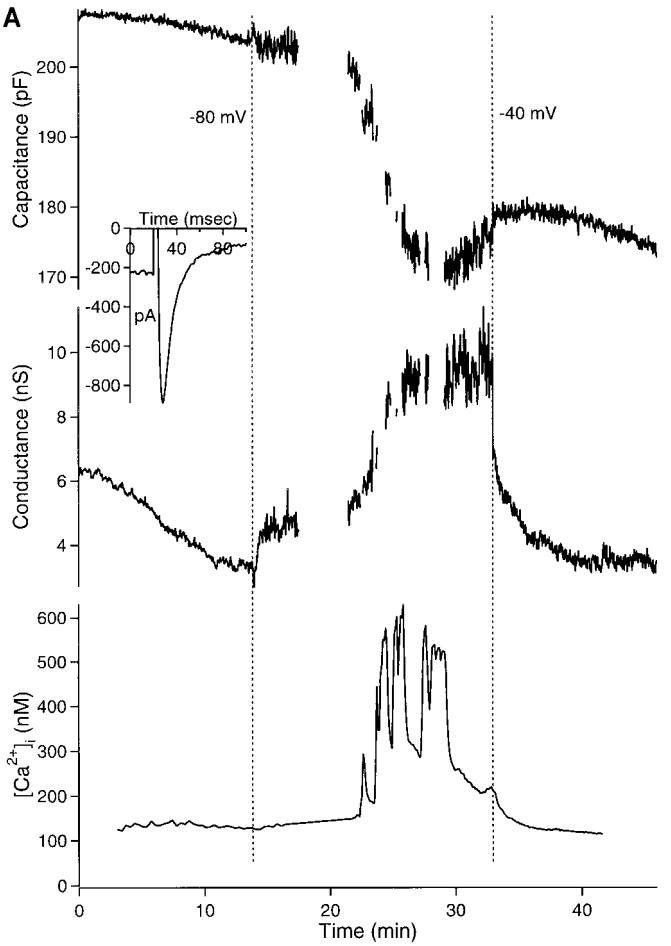

FIG. 10. Forced $[Ca^{2+}]_i$ rise by I_{Ca}. Egg was placed into whole-cell patch configuration with the standard fill solution containing 0.2 mM potassium salt of fura-2 without MgATP. Part A is the entire electrophysiological recording correlated with $[Ca^{2+}]_i$ determined from the central part of the egg (as shown in part B). Changes in holding potential from −40 mV to −80 mV and back occurred at the dashed lines. Starting with the second one, gaps in the capacitance and conductance traces were periods when we invoked the Pulse Train function within the pClamp 7 Membrane Test. Voltage steps 20 ms in duration from −80 to −30 mV were applied every 100 ms for 20–60 s to achieve the $[Ca^{2+}]_i$ increases shown. The inset shows an earlier 80-ms step from −80 to −30 mV; this is a raw current trace with no leak subtraction or any other compensation. Part B shows average $[Ca^{2+}]_i$ determined from the indicated central (dark lower trace) and more peripheral (lighter upper trace) regions of the egg in part A during stimulation of I_{Ca}. Ratio pairs were obtained every 6 s. Bars along the bottom of the graph indicate the approximate periods of I_{Ca} pulse trains, and the numbered points correspond to the false color $[Ca^{2+}]_i$ images arrayed along the bottom. Note that we generally utilized a somewhat larger central region than shown here to determine $[Ca^{2+}]_i$. Bath was the simple saline.

Copyright © 2001 by Academic Press. All rights of reproduction in any form reserved.

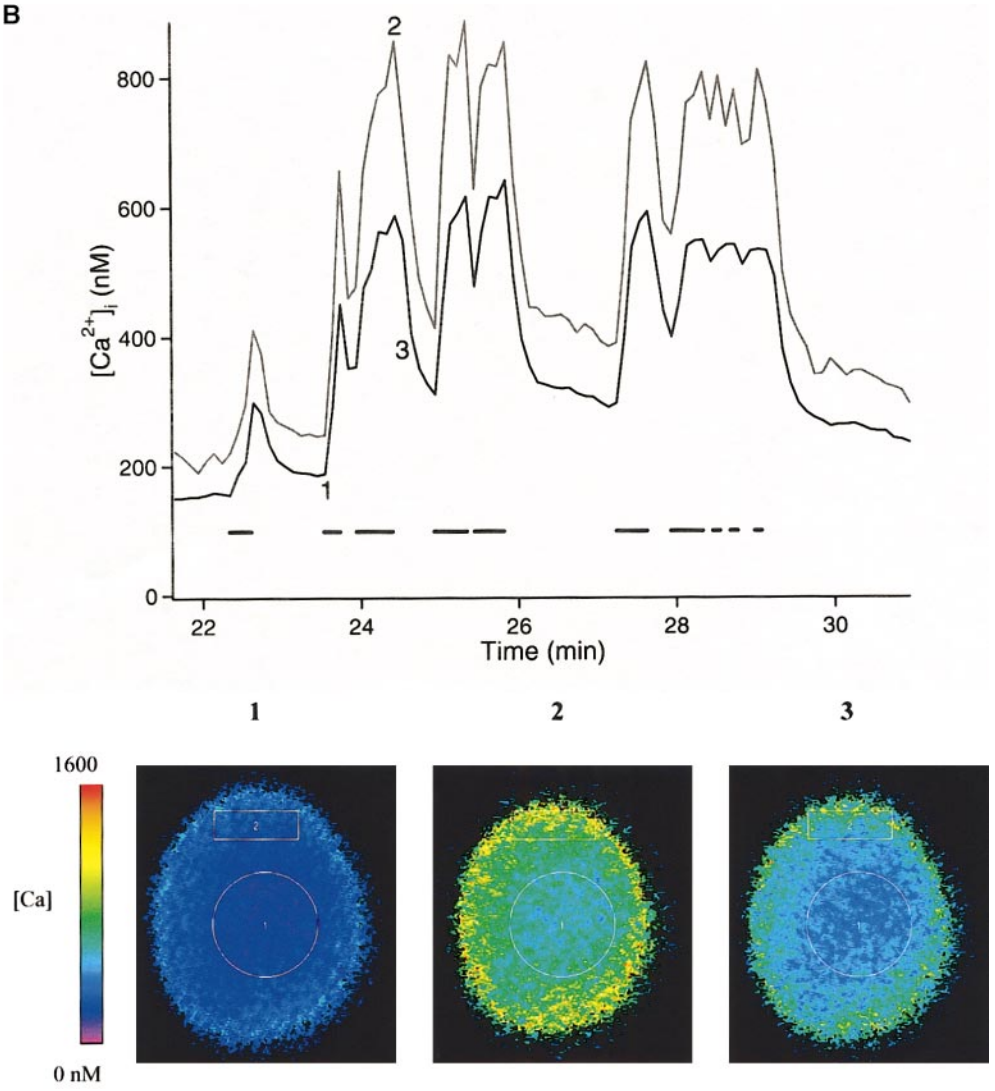

FIG. 10—*Continued*

It is believed that the sperm activates the phosphoinositide pathway, and this results in the production of other products in addition to IP_3. In particular, phosphoinositol breakdown would be expected to generate diacylglycerol and activate protein kinase C. Other work has shown that activation of protein kinase C can lead to cortical granule discharge in mammalian eggs, but the overall activation of the egg is less than that achieved by procedures that raise $[Ca^{2+}]_i$ (Ducibella and LeFevre, 1997; Sun *et al.*, 1997). We added the protein kinase C activator phorbol myristate acetate (PMA) to patch-clamped eggs to see if activation of protein kinase C played a role in the electrophysiological changes. We found that PMA stimulated a decrease in capacitance less than that induced by I_{Ca} with no change in $[Ca^{2+}]_i$ or conductance (data not shown). This suggests that protein kinase C probably plays only a small role in the membrane changes after fertilization. Nevertheless, it might be valuable to investigate the combined effects of PMA and IP_3.

Capacitance Change with I_{Ca} and Ionophore

Raising $[Ca^{2+}]_i$ with I_{Ca} consistently led to a decrease in capacitance. The threshold for capacitance change was about the same as for fertilization and sperm factor. We were unable to force $[Ca^{2+}]_i$ higher than ~900 nM in the egg cortex by this method, so we do not know if higher $[Ca^{2+}]_i$ would have forced a net capacitance increase. There was little increase in conductance associated with raising $[Ca^{2+}]_i$ with I_{Ca}. There was no evidence that raising $[Ca^{2+}]_i$ with I_{Ca}

Copyright © 2001 by Academic Press. All rights of reproduction in any form reserved.

led to the release of intracellular Ca^{2+} stores, as $[Ca^{2+}]_i$ levels decreased as soon as I_{Ca} pulses were stopped.

Ionophore produced very sharp increases in $[Ca^{2+}]_i$ that were very difficult to control and generally deleterious to the cell. As far as we could ascertain, ionophore produced changes in capacitance and conductance that were similar to those produced by fertilization and sperm factor. As with IP_3, the threshold for activation of capacitance and conductance changes was at higher $[Ca^{2+}]_i$ levels (Table 4), but this may be an artifact of slow sampling.

Ca^{2+} Handling

Two aspects of Ca^{2+} handling were different in patch-clamped eggs. First, the length of the initial $[Ca^{2+}]_i$ increase after fertilization was longer than expected, and its rate of rise may have been slower. This could be the result of the intracellular introduction of Ca^{2+} chelators (EGTA, fura-2) from the patch pipet, but the concentrations used were quite minimal (generally $<$1.3 mM), and there was no correlation with the length of time of intracellular perfusion from the pipet. In other cell systems (e.g., Lee and Pappone, 1999), higher EGTA (10 mM) was a poor buffer of intracellular Ca^{2+} during stimulation that releases Ca^{2+} from internal stores. There might be interference with the production and/or action of IP_3 to release Ca^{2+} from intracellular stores, but this seemed to work when IP_3 was introduced directly. Eggs fertilized in perforated-patch configuration, without internal perfusion, may have behaved similarly, but we had very few examples with this technique. We would not expect the voltage clamp to be perturbing as the membrane potential of mouse eggs changes very little during fertilization (Igusa *et al.*, 1983; Jaffe *et al.*, 1983). We tried variations on the pipet fill solution (Cl^- for aspartate$^-$, 0 or 10 mM EGTA, with or without ATP), but all our successful fertilizations ended up having used the same fill solution with 1 mM ATP and high [aspartate]. In sperm-factor and IP_3 experiments, we found no differences when ATP was left out of the fill solution. We also had similar results in some IP_3 experiments with all-Cl^- fill solution, although we found such eggs to show increasing leak that limited the length of time during which they could be studied. That our bath solutions were very low in bicarbonate and protein could also have had an effect, except that we saw normal Ca^{2+} transients in unpatched eggs under the same conditions. In sum, we do not know why there was lengthening of the initial $[Ca^{2+}]_i$ increase.

The second perturbation of Ca^{2+} handling in patched cells was that the secondary $[Ca^{2+}]_i$ increases were severely attenuated or absent entirely. The initial $[Ca^{2+}]_i$ increase originates at the site of sperm entry, but the secondary $[Ca^{2+}]_i$ increases appear to initiate from a different location in the egg (Kline *et al.*, 1999; Deguchi *et al.*, 2000), suggesting that different mechanisms may be involved in their generation. It is possible to elicit $[Ca^{2+}]_i$ transients while bypassing the sperm requirement entirely by introducing IP_3 in mouse eggs by injection (Kline and Kline, 1994) or continuous infusion (Swann, 1992), and in a mouse oocyte by photorelease of caged IP_3 while voltage clamping (Peres *et al.*, 1991). In our hands, infusion of IP_3 produced only the first $[Ca^{2+}]_i$ increase. Again, we were unable to develop an explanation for this.

Are we seeing net capacitance decrease because it is the normal pattern of response, or is it an aberration produced by invasive methods or a deficit in the physiological conditions? Endocytosis is surely a normal part of the process, but the differences in Ca^{2+} handling in patch-clamped cells vs our expectations from the literature and our own observations of unpatched, fertilized eggs raise the possibility that we may have unmasked endocytotic phenomena that would not otherwise stand out. Subtle changes in the eggs produced by voltage clamp and/or internal dialysis may eventually provide insight into normal physiology.

Conductance Change

The only previous electrophysiological observations of fertilization in mouse eggs used microelectrode impalement to monitor membrane potential and membrane resistance (Igusa *et al.*, 1983; Jaffe *et al.*, 1983). Jaffe *et al.* observed a 4-mV hyperpolarization lasting ~1 min shortly after insemination and an overall decrease in membrane resistance with no other change in membrane potential over ~60 min. Igusa *et al.* saw similarly small hyperpolarizations that lasted ~8.5 s and occurred at regular intervals after insemination; they also observed a slow overall hyperpolarization of ~20 mV over 40 min that they believed was primarily due to a K^+ permeability.

In our experiments, conductance increases occurred regularly as part of egg activation, but the new as well as the net current was almost always inward, or depolarizing, from the holding potential of −40 mV. Only in two or three instances did we observe a brief net hyperpolarizing current reminiscent of the Ca^{2+}-activated K^+ current that is so prominent in golden hamster eggs (Miyazaki and Igusa, 1982). The major component of the postactivation conductance increase had a reversal potential ~−35 mV (Fig. 9). Under our conditions, this is very close to the reversal potential for Cl^-, suggesting that an increase in Cl^- conductance could be involved. Indeed, we are making an educated guess when we use 35 mM Cl^- in our pipet fill solutions. If intracellular [Cl^-] were less than this (e.g., 25 mM), then increases in Cl^- conductance would be sufficient to explain both transient hyperpolarizations and long-term hyperpolarization after fertilization.

In many experiments, especially with fertilization or ionophore, a conductance increase occurred more quickly than the presumed Cl^- conductance that activated more slowly after IP_3-induced $[Ca^{2+}]_i$ increase. This earlier-activating conductance was strongly depolarizing. We did not learn anything else about its identity.

Copyright © 2001 by Academic Press. All rights of reproduction in any form reserved.

How Does the Sperm Activate the Egg?

Our data is consistent with the hypothesis that a cytosolic component of the sperm activates the egg after sperm–egg fusion. Sperm factor mimicked all aspects of the $[Ca^{2+}]_i$ increase and capacitance and conductance changes typical of fertilization. Other workers had made similar observations regarding the $[Ca^{2+}]_i$ increase and Ca^{2+}-induced K^+ current in human eggs (Homa and Swann, 1994; Dale *et al.*, 1996).

We observed no changes in $[Ca^{2+}]_i$ or any electrical parameter as a consequence of sperm binding alone, suggesting that sperm fusion is the causal event in mouse egg activation. There were no observed $[Ca^{2+}]_i$ changes of any sort associated with fusion. Instead, there was a lag of ~1 min before any major changes occurred. Although the sperm appears to bring some conductance increase to the egg when the sperm and egg fuse, it is unlikely that this is a significant source of Ca^{2+}. I_{Ca} is a much larger current and brings in substantial Ca^{2+} with no indication that it leads to the release of intracellular Ca^{2+} stores or generalized cell activation.

Our results are consistent with the premise that egg activation is produced solely and exclusively by the action of a factor or factors acting in the egg cytoplasm after sperm–egg fusion. Our data further suggest that sperm factor(s) may do more than initiate the production of IP_3. The fertilization- and sperm factor-initiated pathway is complex and may involve the activation of several signaling mechanisms. Moreover, the activating compound(s) delivered by the sperm may need to be in the correct amount and timing to replicate the full complement of physiological responses. This would be important to keep in mind for future studies that attempt to elucidate the pathways by which fertilization activates the egg.

ACKNOWLEDGMENTS

We thank Prof. Diana Myles and Prof. Paul Primakoff for providing the resources of their lab to support this work. We especially thank Kathryn Kreimborg, Brent Miller, and Jennifer Alfieri for the preparation of mouse gametes, and we thank Brent Miller additionally for many useful discussions. The preparation of boar sperm factor was supported by U.S. Department of Agriculture Grant 2371 (to R.A.F.). This work was supported by National Institutes of Health Grant HD19966 (to R.N.).

REFERENCES

Cole, K. C. (1972). Membranes, Ions and Impulses: A Chapter of Classical Biophysics. University of California Press, Berkeley, CA.

Dale, B., Fortunato, A., Monfrecola, V., and Tosti, E. (1996). A soluble sperm factor gates Ca^{2+}-activated K^+ channels in human oocytes. *J. Assist. Reprod. Gen.* **13,** 573–577.

Darszon, A., Labarca, P., Nishigaki, T., and Espinosa, F. (1999). Ion channels in sperm physiology. *Physiol. Rev.* **79,** 481–510.

Day, M. L., Johnson, M. H., and Cook, D. I. (1998). Cell cycle regulation of a T-type calcium current in early mouse embryos. *Pflügers Arch.* **436,** 834–842.

Deguchi, R., Shirakawa, H., Oda, S., Mohri, T., and Miyazaki, S. (2000). Spatiotemporal analysis of Ca^{2+} waves in relation to the sperm entry site and animal-vegetal axis during Ca^{2+} oscillations in fertilized mouse eggs. *Dev. Biol.* **218,** 299–313, doi:10.1006/dbio.1999.9573.

Ducibella, T., and LeFevre, L. (1997). Study of protein kinase C antagonists on cortical granule exocytosis and cell-cycle resumption in fertilized mouse eggs. *Mol. Reprod. Dev.* **46,** 216–226.

Evans, J. P., and Kopf, G. S. (1998). Molecular mechanisms of sperm–egg interactions and egg activation. *Andrologia* **30,** 297–307.

Faure, J-E., Myles, D. G., and Primakoff, P. (1999). The frequency of calcium oscillations in mouse eggs at fertilization is modulated by the number of fused sperm. *Dev. Biol.* **213,** 370–377, dbio.1999.9388.

Georgiou, P., Bountra, C., Bland, K. P., and House, C. R. (1984). Calcium action potentials in unfertilized eggs of mice and hamsters. *Q. J. Exp. Physiol.* **69,** 365–380.

Georgiou, P., Bountra, C., and House, C. R. (1987). Intracellular and whole-cell recordings from zona-free hamster eggs: Significance of leak impalement artifact. *Q. J. Exp. Physiol.* **72,** 105–118.

Gianaroli, L., Tosti, E., Magli, C., Iaccarino, M., Ferraretti, A. P., and Dale, B. (1994). Fertilization current in the human oocyte. *Mol. Reprod. Dev.* **38,** 209–214.

Grynkiewicz, G., Poenie, M., and Tsien, R. Y. (1985). A new generation of Ca^{2+} indicators with greatly improved fluorescence properties. *J. Biol. Chem.* **260,** 3440–3450.

Hogan, B., Costantini, F., and Lacy, E. (1986). Manipulating the Mouse Embryo: A Laboratory Manual. Cold Spring Harbor Laboratory Press, Cold Spring Harbor, NY.

Homa, S. T., and Swann, K. (1994). A cytosolic sperm factor triggers calcium oscillations and membrane hyperpolarizations in human oocytes. *Hum. Reprod.* **9,** 2356–2361.

Igusa, Y., Miyazaki, S., and Yamashita, N. (1983). Periodic hyperpolarizing responses in hamster and mouse eggs fertilized with mouse sperm. *J. Physiol. (London)* **340,** 633–647.

Jaffe, L. A. (1976). Fast block to polyspermy in sea urchin eggs is electrically mediated. *Nature* **261,** 68–71.

Jaffe, L. A., Sharp, A. P., and Wolf, D. P. (1983). Absence of an electrical polyspermy block in the mouse. *Dev. Biol.* **96,** 317–323.

Jaffe, L. F. (1983). Sources of calcium in egg activation: a review and hypothesis. *Dev. Biol.* **99,** 265–276.

Jones, K. T., Matsuda, M., Parrington, J., Katan, M., and Swann, K. (2000). Different Ca^{2+}-releasing abilities of sperm extracts compared with tissue extracts and phospholipase C isoforms in sea urchin egg homogenate and mouse eggs. *Biochem. J.* **346,** 743–749.

Jones, K. T., Soeller, C., and Cannell, M. B. (1998). The passage of Ca^{2+} and fluorescent markers between the sperm and egg after fusion in the mouse. *Development* **125,** 4627–4635.

Kline, D. (1986). A direct comparison of the extracellular currents observed in the activating frog Xenopus-laevis egg with the vibrating probe and patch-clamp techniques. In "Progress in Clinical and Biological Research, Vol. 210. Ionic Currents in Development; Satellite Meeting to the Tenth International Congress of the International Society of Developmental Biologists" (R. Nuccitelli, Ed.), pp. 189–196. A. R. Liss, New York.

Copyright © 2001 by Academic Press. All rights of reproduction in any form reserved.

Kline, D., and Kline, J. T. (1992). Repetitive calcium transients and the role of calcium in exocytosis and cell cycle activation in the mouse egg. *Dev. Biol.* **149,** 80–89.

Kline, D., Mehlmann, L., Fox, C., and Terasaki, M. (1999). The cortical endoplasmic reticulum (ER) of the mouse egg: localization of ER clusters in relation to the generation of repetitive calcium waves. *Dev. Biol.* **215,** 431–442, dbio.1999.9445.

Kline, D., and Stewart-Savage, J. (1994). The timing of cortical granule fusion, content dispersal, and endocytosis during fertilization of the hamster egg: An electrophysiological and histochemical study. *Dev. Biol.* **162,** 277–287.

Kline, J. T., and Kline, D. (1994). Regulation of intracellular calcium in the mouse egg: Evidence for inositol trisphosphate-induced calcium release, but not calcium-induced calcium release. *Biol. Reprod.* **50,** 193–203.

Lawrence, Y., Whitaker, M., and Swann, K. (1997). Sperm–egg fusion is the prelude to the initial Ca^{2+} increase at fertilization in the mouse. *Development* **124,** 233–241.

Lee, S. C., and Pappone, P. A. (1999). ATP can stimulate exocytosis in rat brown adipocytes without apparent increases in cytosolic Ca^{2+} or G protein activation. *Biophys. J.* **76,** 2297–2306.

McCulloh, D. H., Rexroad, C. E. Jr., and Levitan, H. (1983). Insemination of rabbit eggs is associated with slow depolarization and repetitive diphasic membrane potentials. *Dev. Biol.* **95,** 372–377.

McCulloh, D. H, and Chambers, E. L. (1992). Fusion of membranes during fertilization: increases of the sea urchin egg's membrane capacitance and membrane conductance at the site of contact with the sperm. *J. Gen. Physiol.* **99,** 137–175.

Miyazaki, S., and Igusa, Y. (1981). Fertilization potential in golden hamster eggs consists of recurring hyperpolarizations. *Nature* **290,** 702–704.

Miyazaki, S., and Igusa, Y. (1982). Ca-mediated activation of a K current at fertilization of golden hamster eggs. *Proc. Natl. Acad. Sci. USA* **79,** 931–935.

Miyazaki, S., Shirakawa, H., Nakada, K., and Honda, Y. (1993). Essential role of the inositol 1,4,5-trisphosphate receptor/Ca^{2+} release channel in Ca^{2+} waves and Ca^{2+} oscillations at fertilization of mammalian eggs. *Dev. Biol.* **158,** 62–78.

Oda, S., Deguchi, R., Mohri, T., Shikano, T., Nakanishi, S., and Miyazaki, S. (1999). Spatiotemporal dynamics of the $[Ca^{2+}]_i$ rise induced by microinjection of sperm extract into mouse eggs: Preferential induction of a Ca^{2+} wave from the cortex mediated by the inositol 1,4,5-trisphosphate receptor. *Dev. Biol.* **209,** 172–185, dbio.1999.9233.

Okamoto, H., Takahashi, K., and Yamashita, N. (1977). Ionic currents through the membrane of the mammalian oocyte and their comparison with those in the tunicate and sea urchin. *J. Physiol. (London)* **267,** 465–495.

Peres, A. (1986). Resting membrane potential and inward current properties of mouse ovarian oocytes and eggs. *Pflügers Arch.* **407,** 534–544.

Peres, A. (1987). The calcium current of mouse egg measured in physiological calcium and temperature conditions. *J. Physiol. (London)* **391,** 573–588.

Peres, A., Bertollini, L., and Racca, C. (1991). Characterization of Ca^{2+} transients induced by intracellular photorelease of $InsP_3$ in mouse ovarian oocytes. *Cell Calcium* **12,** 457–465.

Sun, Q-Y., Wang, W-H., Hosoe, M., Taniguchi, T., Chen, D-Y., and Shioya, Y. (1997). Activation of protein kinase C induces cortical granule exocytosis in a Ca^{2+}-independent manner, but not the resumption of cell cycle in porcine eggs. *Dev. Growth Differ.* **39,** 523–529.

Swann, K. (1990). A cytosolic sperm factor stimulates repetitive calcium increases and mimics fertilization in hamster eggs. *Development* **110,** 1295–1302.

Swann, K. (1992). Different triggers for calcium oscillations in mouse eggs involve a ryanodine-sensitive calcium store. *Biochem. J.* **287,** 79–84.

Tahara, M., Tasaka, K., Masumoto, N., Mammoto, A., Ikebuchi, Y., and Miyake, A. (1996). Dynamics of cortical granule exocytosis at fertilization in living mouse eggs. *Am. J. Physiol.* **270,** C1354–C1361.

Wu, H., He, C. L., and Fissore, R. A. (1997). Injection of a porcine sperm factor triggers calcium oscillations in mouse oocytes and bovine eggs. *Mol. Reprod. Dev.* **46,** 176–189.

Wu, H., He, C. L., and Fissore, R. A. (1998). Injection of a porcine sperm factor induces activation of mouse eggs. *Mol. Reprod. Dev.* **49,** 37–47.

Received for publication September 13, 2000
Revised December 4, 2000
Accepted January 5, 2001
Published online February 27, 2001

Copyright © 2001 by Academic Press. All rights of reproduction in any form reserved.